

BACHELOR'S THESIS

One-Loop Contributions to the
Muon $(g - 2)$ Anomaly in the
Two-Higgs-Doublet Model

Submitted by
Daniel Christian Woitaschek

September 23, 2024

First examiner
Prof. Dr. Michael Klasen

Second examiner
PD. Dr. Karol Kovařík

University of Münster
Institute for Theoretical Physics

Contents

1	Introduction	2
2	The Anomalous Magnetic Moment in the Standard Model	3
2.1	The Landé g -Factor	3
2.2	Measurement of the Anomalous Magnetic Moment of the Muon	3
2.3	From the Dirac Equation to the Pauli Equation	5
2.4	Tree-Level Contribution	7
2.5	Electromagnetic Form Factors	10
2.6	One-Loop QED Contribution	12
3	Electroweak One-Loop Contributions for Scalar-Fermion Interactions	17
3.1	The Anomalous Magnetic Moment in Arbitrary Scalar-Fermion Interaction Models	17
3.2	Photon Absorption from the Internal Scalar Line	18
3.3	Photon Absorption from the Internal Fermion Line	22
4	The Two-Higgs-Doublet Model	22
4.1	Introduction to the Two-Higgs-Doublet Model	22
4.2	The Anomalous Magnetic Moment for Different Textures of Yukawa Couplings . .	24
4.2.1	Texture 1: Muon-Muon Yukawa Coupling Matrix	25
4.2.2	Texture 2: Tau-Muon Yukawa Coupling Matrix	28
4.2.3	Texture 3: Muon-Tau and Tau-Muon Yukawa Coupling Matrix	31
4.2.4	Texture 4: Muon-Electron Yukawa Coupling Matrix	33
4.2.5	Direct Comparison of the Parameter Spaces	35
5	Conclusion	37
	Appendix A Appendix	38
A.1	Gamma Matrices	38
A.2	Feynman Rules	39
A.3	Gordon Identity	39
A.4	Feynman Parametrization	40
A.5	Dimensional Regularization and Wick rotations	41
A.6	Reproduction of the Electroweak Contributions Using <i>package-X</i>	42
A.7	Explicit Calculation of the Mass Matrix	45
A.8	Left- and Right Handed Projection Operators	47

1 Introduction

The field of particle physics strives for the revelation of the most fundamental laws of nature. Its most successful theory, the Standard Model (SM), allowed an outstandingly accurate prediction of several phenomena at the smallest scales of physics. The Standard Model describes fermions, the generators of matter, and bosons, the mediators of interactions between fermions. The latest great triumph of the standard model was the correct prediction of the Higgs boson that was detected in 2012 [1]. Despite the great success of this theory, there is a broad consensus that the Standard Model is still incomplete. Several phenomena can not be explained with the current capabilities of the SM, one of which is the muon ($g - 2$) anomaly, referring to the anomalous magnetic moment (AMM) of the muon. The spin magnetic moment $\boldsymbol{\mu}_s$ of the muon is given as:

$$\boldsymbol{\mu}_s = -g \frac{e}{2m} \mathbf{S}.$$

The Landé g -factor describes the proportionality between the magnetic moment and the spin \mathbf{S} . The AMM refers to deviations of the g -factor from being precisely two and is defined as:

$$a_\mu = \frac{g - 2}{2}.$$

The connection to particle physics is made with the description of the AMM in the context of quantum field theory. Within this theory, the AMM is caused by loop corrections to the tree level Feynman diagram. Consequently, the AMM is characterized by the interactions with virtual particles within the loop, therefore marking a touchstone for the current state of the SM. The value of the AMM was both experimentally measured and theoretically calculated. The most recent experimental value from Fermi National Laboratory (Fermilab) leads to a current experimental average of $a_\mu(\text{Exp}) = 116592059(22) \cdot 10^{-11}$ [2] (August 2023). The current SM prediction states a value of $a_\mu(\text{SM}) = 116591810(43) \cdot 10^{-11}$ [3] (December 2020). This leads to a discrepancy of [4]

$$\Delta a_\mu = a_\mu(\text{Exp}) - a_\mu(\text{SM}) = (2.49 \pm 0.483) \cdot 10^{-9},$$

which turns out to be a deviation of 5.1σ . By convention, a deviation of more than 5σ is regarded as a new discovery in particle physics. This difference between the theoretical and the experimental value opens up room for theories of new physics beyond the SM that explain the missing contribution.

A promising theory to resolve this anomaly is the two-Higgs-doublet model (2HDM), which is motivated by the concept of the Minimal Supersymmetric Standard Model (MSSM) [5]. The 2HDM extends the scalar sector of the SM and predicts the existence of a second SU(2) Higgs doublet. The new doublet generates a total of three additional scalar contributions. Including the electroweak interactions of these particles with the muon at one-loop level allows an explanation of the missing contribution for an agreement with Δa_μ .

After a brief summary of the experimental measurement of the AMM, the calculations that lead to a value of $g = 2$ are retraced. First, the Dirac equation is transformed into the Pauli equation which allows a direct derivation of the Landé factor. Second, the contribution of $g = 2$ is obtained in the framework of quantum field theory by extracting the g -factor from the transition amplitude at tree level. Subsequently, the one-loop contribution from quantum electrodynamics (QED) is calculated, resulting in the largest contribution to the AMM of $a_\mu = \alpha/2\pi$ that was famously calculated by Julian Schwinger [6].

In the next step, a generalized electroweak one-loop calculation is performed which allows the application of arbitrary scalar-fermion interaction models. For this, two scalar-fermion interaction topologies are considered. In the first scenario, the photon from the external electromagnetic field is absorbed by an internal charged scalar in the loop. In the second scenario, the photon is absorbed by an internal charged fermion in the loop. The first scenario is calculated in detail whereas the second calculation is reproduced with *package-X* in *Mathematica* [7].

The last chapter adapts the obtained results to the 2HDM. In total, four different Yukawa coupling textures are analyzed. For each case, a parameter space scan is conducted to find parameter combinations for the Yukawa coupling and the scalar mass that can resolve the muon ($g - 2$) anomaly. Moreover, experimentally excluded regions are embedded into the parameter space to indicate further constraints on the properties of the scalars, which subsequently allows a more targeted experimental search after the new scalar particles.

2 The Anomalous Magnetic Moment in the Standard Model

The first part of this work retraces the steps that lead up to the one-loop QED contribution to the AMM. Throughout all calculations, we use the natural unit system in which $c = \hbar = 1$ holds. Three-component vectors are printed in **bold**.

2.1 The Landé g -Factor

The magnetic moment $\boldsymbol{\mu}$ is classically given as

$$\boldsymbol{\mu} = I \cdot \mathbf{A} = I \cdot A \cdot \mathbf{n}, \quad (2.1)$$

where \mathbf{A} is the area which is enclosed by a charge current I . The vector \mathbf{n} points in the normal direction of the area. Considering a charged rotating particle with charge q and a rotatory frequency f we can rewrite the charge current as

$$I = \frac{q}{T} = q \cdot f \quad \text{with} \quad f = \frac{v}{2\pi r}, \quad (2.2)$$

with the tangent velocity v and the radius r . The magnetic moment can thus be specified with the area of a circle as

$$\boldsymbol{\mu} = q \cdot \frac{v}{2\pi r} \cdot \pi r^2 \mathbf{n} \cdot \frac{m}{m} = \frac{q}{2m} \mathbf{L} \quad (2.3)$$

which allows us to identify the classical angular momentum $\mathbf{L} = m \cdot \mathbf{r} \cdot \mathbf{v} \cdot \mathbf{n}$.

In quantum mechanics, the total angular momentum \mathbf{J} is given as a sum of the orbital angular momentum \mathbf{L} and the spin \mathbf{S} leading to

$$\boldsymbol{\mu} = \frac{q}{2m} (\mathbf{L} + g\mathbf{S}). \quad (2.4)$$

The g -factor is introduced (also called the Landé g -factor) to account for possible deviations due to the transition from classical mechanics to the quantum domain since \mathbf{S} does not have a classical analogue.

2.2 Measurement of the Anomalous Magnetic Moment of the Muon

The following section provides an overview of the experimental determination of a_μ highlighting the physical principles that allow the precise measurement at Fermilab [2]. The following explanations are based on [8] and describe the experimental setup that was originally used at the Brookhaven National Laboratory (BNL). The BNL storage ring was relocated to Fermilab in 2013 so the fundamental principles remain valid.

In the BNL experiment, the AMM of positive muons was determined (Fig. 1). The positively charged muons are produced as a result of the pion decay $\pi^+ \rightarrow \mu^+ \nu_\mu$. The pions in turn are produced by high energetic protons from the Alternating Gradient Synchrotron (AGS) that hit a target. The muons emitted are polarized, meaning that the spins point in the same direction as the momenta. The muons are then injected into the storage ring in which a uniform magnetic field \mathbf{B} is applied. Due to the Lorentz force, the muons move in a circular orbit around the ring and are accelerated to relativistic velocities. They orbit the ring with a cyclotron frequency $\boldsymbol{\omega}_c$ of

$$\boldsymbol{\omega}_c = \frac{e\mathbf{B}}{m\gamma} \quad (2.5)$$

where $\gamma = \sqrt{1 - v^2/c^2}$ is the relativistic Lorentz factor. Moreover, the spin axis of the muon precesses around the axis of the magnetic field known as Larmor precession. The Larmor frequency of this precession $\boldsymbol{\omega}_s$ is given as [9]

$$\boldsymbol{\omega}_s = g \frac{e\mathbf{B}}{2m} + (1 - \gamma) \frac{e\mathbf{B}}{m\gamma}. \quad (2.6)$$

2 The Anomalous Magnetic Moment in the Standard Model

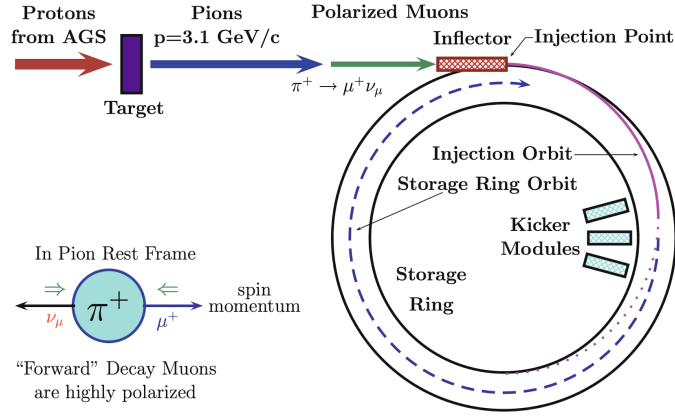


Figure 1: Simplified schematic illustration of the experimental setup originally used at the Brookhaven National Laboratory (BNL) as well a visualization of the parity violating pion decay. Taken from [8].

The second term emerges from the Thomas precession, a relativistic correction to the Lamor precession. The AMM can be obtained from the difference frequency ω_a of the Lamor and cyclotron frequency:

$$\begin{aligned}
 \omega_a &= \omega_s - \omega_c \\
 &= g \frac{e\mathbf{B}}{2m} + (1 - \gamma) \frac{e\mathbf{B}}{m\gamma} - \frac{e\mathbf{B}}{m\gamma} \\
 &= \frac{e\mathbf{B}}{m} \left(\frac{g-2}{2} \right) \\
 &= a_\mu \frac{e\mathbf{B}}{m}. \tag{2.7}
 \end{aligned}$$

Here, it becomes also evident why the factor of 1/2 appears in the definition of a_μ . The magnetic field \mathbf{B} is also measured in this experiment, while e and m are determined in independent experiments. If g was exactly equal to two, the cyclotron frequency and the Lamor frequency would be equal. In conclusion, the AMM causes a misalignment between the direction of motion and the spin axis, as can be seen in Fig. 2.

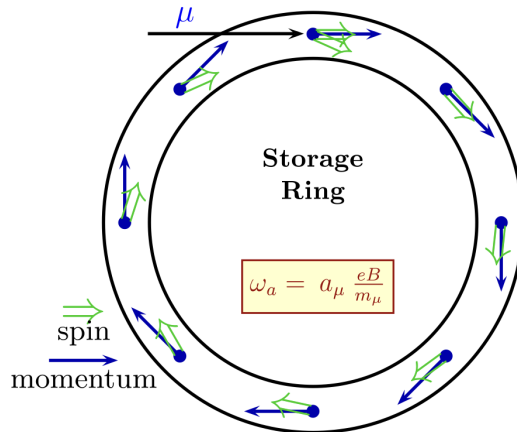


Figure 2: Schematic illustration of the spin and momentum orientation during one circulation in the cyclotron. Taken from [10].

The remaining challenge is to determine the spin direction. For that, the parity violating decay of the muon into a positron of $\mu^+ \rightarrow e^+ + \nu_e + \bar{\nu}_\mu$ is analyzed. The parity violation causes the emission

2 The Anomalous Magnetic Moment in the Standard Model

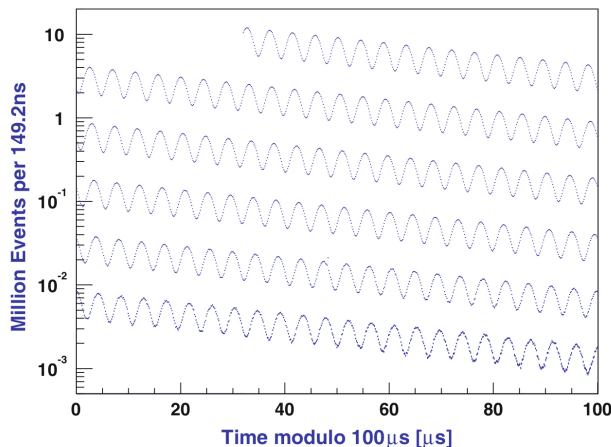


Figure 3: Time distribution of the detected positrons with $E > E_{\text{th}}$ for different E_{th} . The frequency of the signal matches ω_a . Retrieved from [8].

direction of the positron to be highly correlated to the spin axis. The positrons are detected by 24 equidistant calorimeters, which measure the positrons energy and therefore reveal information about the spin orientation. The number $N(t)$ of detected positrons above a threshold energy E_{th} is given as:

$$N(t) = N_0(E_{\text{th}}) \exp\left(\frac{-t}{\gamma\tau_\mu}\right) (1 + A(E_{\text{th}}) \sin(\omega_a t + \phi(E_{\text{th}}))) \quad (2.8)$$

with the muon-lifespan τ_μ , the asymmetry factor of the decay A and the phase factor ϕ . The quintessence to conclude from this expression is that the decay of the muons is modulated with the frequency ω_a from which a_μ can be determined. The detected signal takes a form as it is depicted in Fig. 3.

2.3 From the Dirac Equation to the Pauli Equation

Now, the g -factor is derived in the framework of relativistic quantum mechanics (based on [11], P.59-73). In order to describe relativistic particles, a generalization of the Schrödinger equation has to be found in which Lorentz invariance is preserved. In order to do so, the Lorentz invariant energy-momentum relation has to be taken into account:

$$E^2 = m^2 + p^2. \quad (2.9)$$

Following the correspondence principle of quantum mechanics, we can insert the operator representations of $E = i\partial_t$ and $p = -i\nabla$ (under the assumption that they act on a wavefunction $\psi(\mathbf{r}, t)$) to arrive at the Klein-Gordon equation:

$$(\partial_t^2 - \nabla^2 - m)\psi(\mathbf{r}, t) = 0. \quad (2.10)$$

One can observe that this second-order differential equation requires two initial conditions. By a linearization, the Klein-Gordon equation can be reduced to a first order differential equation leading to the Dirac equation of a free particle:

$$(i\partial_t + \underbrace{i\boldsymbol{\alpha}\nabla - \beta m}_{H_D})\psi(\mathbf{r}, t) = 0 \quad (2.11)$$

H_D is our identified time-independent Dirac-Hamiltonian. The parameters $\boldsymbol{\alpha}$ and β are assumed to take the shape of a squared matrix for reasons that become evident in a moment. To incorporate spin into this formalism, the wave functions are promoted to spinors of the form:

$$|\psi\rangle = \begin{pmatrix} \psi_1 \\ \psi_2 \\ \psi_3 \\ \psi_4 \end{pmatrix} = \begin{pmatrix} \psi_A \\ 0 \end{pmatrix} + \begin{pmatrix} 0 \\ \psi_B \end{pmatrix} \quad \text{with} \quad \psi_A = \begin{pmatrix} \psi_1 \\ \psi_2 \end{pmatrix}, \quad \psi_B = \begin{pmatrix} \psi_3 \\ \psi_4 \end{pmatrix}. \quad (2.12)$$

2 The Anomalous Magnetic Moment in the Standard Model

In the non-relativistic limit $p \ll m$, ψ_A is much larger than ψ_B . This is because ψ_B can be replaced by

$$|\psi\rangle = \begin{pmatrix} \psi_A \\ \psi_B \end{pmatrix} = \begin{pmatrix} \psi_A \\ \frac{\boldsymbol{\sigma} \cdot \mathbf{p}}{E+m} \psi_A \end{pmatrix} \quad (2.13)$$

for a free particle. In this limit, the lower component vanishes and we arrive at an effective two-component theory. The upper components ψ_A are often denoted as the large components whereas ψ_B refers to the small components.

$$|\psi\rangle = |\psi_A\rangle \quad (2.14)$$

Up to this point, the Dirac-equation of a free particle was discussed. When it comes to the extraction of the magnetic moment, the Dirac-Hamiltonian subsequently has to be modified. In general, the Hamiltonian arising from a magnetic interaction is given as:

$$H_B = -\boldsymbol{\mu} \cdot \mathbf{B} = g \frac{e}{4m} (\boldsymbol{\sigma} \cdot \mathbf{B}). \quad (2.15)$$

This result was gained from the fact that the spin operator from Eq. 2.4 is directly proportional to the Pauli-matrices via:

$$\mathbf{S} = \frac{1}{2} \boldsymbol{\sigma}. \quad (2.16)$$

The goal is now to find the Dirac Hamiltonian for a charged particle in an electromagnetic field, in which we can identify the magnetic interaction Hamiltonian and therefore determine the required g -factor. In order to account for the interaction with an electromagnetic field we apply the substitutions of

$$\mathbf{p} \rightarrow \mathbf{p} + e\mathbf{A} \quad \text{and} \quad E \rightarrow E + e\phi, \quad (2.17)$$

to Eq. 2.11 with the scalar electric potential ϕ and the magnetic vector potential \mathbf{A} . These substitutions result in the Dirac Hamiltonian H_D for a charged particle in an electromagnetic field:

$$H_D = \boldsymbol{\alpha}(\mathbf{p} + e\mathbf{A}) + \beta m - e\phi. \quad (2.18)$$

The requirements for $\boldsymbol{\alpha}$ and β are that:

$$\{\alpha_i, \alpha_j\} = 2\delta_{ij}\mathbb{1}, \quad \{\alpha_i, \beta\} = 0, \quad \beta^2 = \mathbb{1}. \quad (2.19)$$

These conditions are satisfied by the γ -matrices (Appendix A.1). H_D therefore becomes

$$H_D = \boldsymbol{\gamma}(\mathbf{p} + e\mathbf{A}) + \gamma^0 m + e\phi\mathbb{1}. \quad (2.20)$$

We will now act this Hamiltonian on a Dirac spinor:

$$\begin{aligned} H_D \begin{pmatrix} \psi_A \\ \psi_B \end{pmatrix} &= (\mathbf{p} + e\mathbf{A}) \begin{pmatrix} 0 & \boldsymbol{\sigma} \\ \boldsymbol{\sigma} & 0 \end{pmatrix} \begin{pmatrix} \psi_A \\ \psi_B \end{pmatrix} + m \begin{pmatrix} \mathbb{1} & 0 \\ 0 & -\mathbb{1} \end{pmatrix} \begin{pmatrix} \psi_A \\ \psi_B \end{pmatrix} - e\phi \begin{pmatrix} \psi_A \\ \psi_B \end{pmatrix} \\ &= (\mathbf{p} + e\mathbf{A}) \begin{pmatrix} \boldsymbol{\sigma}\psi_B \\ \boldsymbol{\sigma}\psi_A \end{pmatrix} + m \begin{pmatrix} \psi_A \\ -\psi_B \end{pmatrix} - e\phi \begin{pmatrix} \psi_A \\ \psi_B \end{pmatrix} \stackrel{!}{=} E \begin{pmatrix} \psi_A \\ \psi_B \end{pmatrix}. \end{aligned} \quad (2.21)$$

Expanding this leads to the following system of equations:

$$(\mathbf{p} + e\mathbf{A}) \cdot \boldsymbol{\sigma}\psi_B = (E - m + e\phi)\psi_A \quad (2.22)$$

$$(\mathbf{p} + e\mathbf{A}) \cdot \boldsymbol{\sigma}\psi_A = (E + m + e\phi)\psi_B. \quad (2.23)$$

For ψ_B we can rearrange the expression to:

$$\psi_B = \frac{(\mathbf{p} + e\mathbf{A}) \cdot \boldsymbol{\sigma}\psi_A}{(E + m + e\phi)}. \quad (2.24)$$

Under the assumption that the influence of the electric field to the total energy is sufficiently small ($e\phi \ll m$), we gain the following simplification:

$$\psi_B = \frac{1}{2m} (\mathbf{p} + e\mathbf{A}) \cdot \boldsymbol{\sigma}\psi_A. \quad (2.25)$$

2 The Anomalous Magnetic Moment in the Standard Model

As already discussed, we are interested in the non-relativistic limit of the Dirac-theory known as the Pauli-theory. For that reason, it is sufficient to only consider the large component ψ_A of Eq. 2.23. Plugging in Eq. 2.25 yields:

$$\underbrace{\left(\frac{1}{2m}((\mathbf{p} + e\mathbf{A}) \cdot \boldsymbol{\sigma})(\mathbf{p} + e\mathbf{A}) \cdot \boldsymbol{\sigma}) - e\phi\right)}_{H_p} \psi_A = (E - m)\psi_A, \quad (2.26)$$

where we defined H_p as the Pauli Hamiltonian. The Pauli Hamiltonian can be rearranged in order to extract the magnetic moment to

$$H_p = \frac{1}{2m}((\mathbf{p} + e\mathbf{A})^2 + i\boldsymbol{\sigma} \cdot (\mathbf{p} + e\mathbf{A}) \times (\mathbf{p} + e\mathbf{A})) - e\phi. \quad (2.27)$$

Here, the following identity was used (proof in Appendix A.1):

$$(\mathbf{a} \cdot \boldsymbol{\sigma})(\mathbf{b} \cdot \boldsymbol{\sigma}) = \mathbf{a} \cdot \mathbf{b} + i\boldsymbol{\sigma}(\mathbf{a} \times \mathbf{b}). \quad (2.28)$$

The underlined term can be reduced in the following way:

$$\begin{aligned} ((\mathbf{p} + e\mathbf{A})\psi_A) \times (\mathbf{p} + e\mathbf{A}) &= \frac{1}{2}\varepsilon_{ijk}[p_j + eA_j, p_k + eA_k]\psi_A \\ &= \frac{-ie}{2}\varepsilon_{ijk}([\partial_j, A_k] + [\partial_k, A_j])\psi_A \\ &= \frac{-ie}{2}\varepsilon_{ijk}(\partial_j A_k - A_k \partial_j + A_j \partial_k - \partial_k A_j)\psi_A \\ &= \frac{-ie}{2}\varepsilon_{ijk}[(\partial_j A_k)\psi_A + A_k(\partial_j \psi_A) - A_k(\partial_j \psi_A) \\ &\quad + A_j(\partial_k \psi_A) - (\partial_k A_j)\psi_A - A_j(\partial_k \psi_A)]\psi_A \\ &= \frac{-ie}{2}\varepsilon_{ijk}(\partial_j A_k - \partial_k A_j)\psi_A \\ &= \frac{-ie}{2}2\varepsilon_{ijk}(\partial_j A_k)\psi_A \\ &= -ie\mathbf{B}\psi_A \end{aligned} \quad (2.29)$$

In the first line we utilized that

$$\begin{aligned} \boldsymbol{\pi} \times \boldsymbol{\pi} &= \varepsilon_{ijk}\pi_j\pi_k = \frac{1}{2}\varepsilon_{ijk}[\pi_j, \pi_k] \\ \text{since } \varepsilon_{ijk}[\pi_j, \pi_k] &= \varepsilon_{ijk}\pi_j\pi_k - \varepsilon_{ijk}\pi_k\pi_j = \varepsilon_{ijk}\pi_j\pi_k + \varepsilon_{ijk}\pi_j\pi_k = 2\varepsilon_{ijk}\pi_j\pi_k. \end{aligned} \quad (2.30)$$

Merging everything together ends up in the following expression for the Pauli-Hamiltonian

$$H_p = \frac{1}{2m}(\mathbf{p} + e\mathbf{A})^2 \mathbb{1} + \frac{e}{2m}(\boldsymbol{\sigma} \cdot \mathbf{B}) - e\phi \mathbb{1} \quad (2.31)$$

A direct comparison with the Hamiltonian of a magnetic interaction in Eq. 2.15 illustrates $g = 2$ in the relativistic formulation of quantum mechanics.

2.4 Tree-Level Contribution

The subsequent section focuses on the extraction of the g value from a tree-level scattering process using perturbation theory to verify the consistency with the results discussed in the previous chapter. This section is based on [12], P.117-119. The tree-level diagram takes the following form:

2 The Anomalous Magnetic Moment in the Standard Model

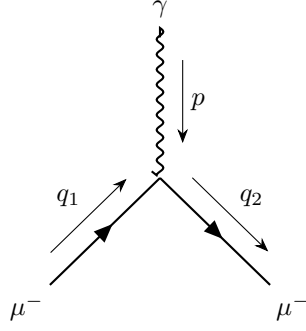


Figure 4: Topology of the tree-level Feynman diagram.

The application of the Feynman rules (Appendix A.2) for a simple fermion-photon vertex results in the expression of

$$iM^\mu = -ie\bar{u}(q_2)\gamma^\mu u(q_1). \quad (2.32)$$

Here, $\bar{u}(q_2)$ and $u(q_1)$ are the momentum dependent factors of a plain wave solution of a Dirac spinor $\psi(x)$ given as:

$$\psi(x) = u(q)e^{-iqx} \quad \bar{\psi}(x) = \bar{u}(q)e^{iqx}. \quad (2.33)$$

With the Gordon identity (proof in Appendix A.3), this expression can be extended to

$$iM^\mu = \frac{-ie}{2m}\bar{u}(q_2)((q_2 + q_1)^\mu + i\sigma^{\mu\nu}(q_2 - q_1)_\nu)u(q_1). \quad (2.34)$$

In the following steps, the interest lies on the transition amplitude between the initial state ψ_1 and the final state ψ_2 which can be derived from perturbative considerations. Starting with the Dirac equation of a free particle

$$(\not{p} - m)\psi = 0, \quad (2.35)$$

the inclusion of the interaction with the electromagnetic (EM) four-vector potential $A^\mu = (\phi, \mathbf{A})^T$ is realized by applying the substitution of $p^\mu \rightarrow p^\mu + eA^\mu$:

$$(\gamma_\mu p^\mu - m)\psi = -e\gamma_\mu A^\mu \psi \equiv \gamma^0 V \psi. \quad (2.36)$$

The interaction with the EM potential is defined as a perturbation V . The γ^0 guarantees the correct matrix dimension of the perturbation. One can derive the amplitude for the scattering process T_{21} of the muon, using first-order time dependent perturbation theory

$$\begin{aligned} T_{2,1} &= -i \int_{\mathbb{R}^4} dx^4 \psi^\dagger(x) V(x) \psi(x) \\ &= ie \int_{\mathbb{R}^4} dx^4 \psi^\dagger \gamma_\mu A^\mu \psi \\ &= -i \int_{\mathbb{R}^4} dx^4 j_\mu^{2,1} A^\mu. \end{aligned} \quad (2.37)$$

Here, the transition current was $j_\mu^{2,1}$ was introduced as

$$j_\mu^{2,1} = -e\psi_2^\dagger(x)\gamma_\mu\psi_1(x) = -e\bar{u}(q_2)\gamma_\mu u(q_1) \cdot e^{i(q_2 - q_1) \cdot x} = M_\mu \cdot e^{i(q_2 - q_1)x}. \quad (2.38)$$

This connects the transition amplitude and the the invariant amplitude via:

$$T_{2,1} = -i \int_{\mathbb{R}^4} dx^4 M_\mu A^\mu e^{i(q_2 - q_1)x} \quad (2.39)$$

Under the assumption that A^μ is time-independent the integration of the 0th component can be carried out:

$$T_{2,1} = -2\pi\delta(E_2 - E_1) \int_{\mathbb{R}^3} d^3x j_\mu^{2,1} A^\mu. \quad (2.40)$$

2 The Anomalous Magnetic Moment in the Standard Model

Inserting the transition current and the Gordon identity results in

$$T_{2,1} = -i2\pi\delta(E_2 - E_1) \left(\underbrace{\int d^3x \bar{\psi}_2 \frac{-e}{2m} (q_2 + q_1)_\mu \psi_1 A^\mu}_{I_1} + \underbrace{\int d^3x \bar{\psi}_2 \frac{-e}{2m} i\sigma_{\mu\nu} (q_2 - q_1)^\nu \psi_1 A^\mu}_{I_2} \right). \quad (2.41)$$

I_1 and I_2 are now treated separately. For I_1 we have

$$I_1 = \frac{-e}{2m} \int d^3x \bar{u}(q_2) (q_2 + q_1)_\mu e^{i(q_1 - q_2)x} u(q_1) A^\mu. \quad (2.42)$$

Regarding $\mu = 0$, the δ -function guarantees the energy conservation and sets $E_2 = E_1$. Therefore, the $\mu = 0$ components of the four-momenta q_2 and q_1 are equal and everything can be summarized as

$$I_1^0 = \frac{-e}{2m} \int d^3x \bar{u}(q_2) (2E_2) A^0 u(q_1) e^{i(q_2 - q_1)x}. \quad (2.43)$$

In the non-relativistic limit of $p \rightarrow 0$, $E = m$ holds in the energy-momentum relation (Eq. 2.9) which allows us to cancel out the $2m$ in the denominator such that I_1^0 takes the form of

$$I_1^0 = -e \cdot \int d^3x \bar{\psi}_2^A \phi \mathbb{1} \psi_1^A. \quad (2.44)$$

As another consequence of the non-relativistic limit, the lower components of the Dirac spinors (see Eq. 2.13) are neglected such that only the upper components ψ^A remain.

Now the spatial components $\mu = 1, 2, 3$ are examined (the index μ is labeled to euclidean indices i by the cost of an extra minus sign due to the Minkowski metric).

$$\begin{aligned} I_1^{1,2,3} &= \frac{ie}{2m} \int d^3x \bar{u}(q_2) (\partial_2 + \partial_1)_i e^{i(q_2 - q_1)x} u(q_1) A_i \\ &\stackrel{\text{PR}}{=} \frac{ie}{2m} \int d^3x \underbrace{\bar{u}(q_2) ((\partial_2 + \partial_1)_i (e^{i(q_2 - q_1)x} A_i))}_{I_{1,1}} u(q_1) - \underbrace{\bar{u}(q_2) e^{i(q_2 - q_1)x} ((\partial_2 + \partial_1)_i A_i) u(q_1)}_{I_{1,2}} \end{aligned} \quad (2.45)$$

In the second line, a rearranged form of the product rule was used. Under the establishment of the Coulomb gauge

$$\partial_i \cdot A_i = 0 \quad (2.46)$$

$I_{1,2}$ vanishes. For $I_{1,1}$ we can make use of the Gauss' law to transform a volume integral over a divergence of a vector field to an surface integral:

$$\begin{aligned} I_{1,1} &= \int d^3x \bar{u}(q_2) ((\partial_2 + \partial_1)_i (e^{i(q_2 - q_1)x} A_i)) u(q_1) \\ &= \int d\mathbf{S} \bar{u}(q_2) (e^{i(q_2 - q_1)x} \mathbf{A}) u(q_1). \end{aligned} \quad (2.47)$$

The oscillating functions are bounded. Assuming that \mathbf{A} is finite and vanishes as $x \rightarrow \infty$, the surface integral of $I_{1,2}$ equals zero because the integration is performed over the whole \mathbb{R}^3 which means that the surface is located at infinity.

Now, the examination of I_2 is carried out.

$$I_2 = \int d^3x \bar{\psi}_2 \frac{-e}{2m} i\sigma^{\mu\nu} (q_2 - q_1)_\nu \psi_1 A^\mu \quad (2.48)$$

The time-like component vanishes since $E_2 = E_1$, so only the space-like components survive. With

2 The Anomalous Magnetic Moment in the Standard Model

$p = q_2 - q_1$ and the euclidean indices i, j, k it follows that

$$\begin{aligned}
 I_2^{1,2,3} &= \frac{e}{2m} \int d^3x \bar{u}(q_2) \sigma_{ij} \partial_j e^{ipx} u(q_1) A_i \\
 &\stackrel{\text{PR}}{=} \frac{e}{2m} \int d^3x \bar{u}(q_2) \sigma_{ij} \partial_j (e^{ipx} A_i) - \bar{u}(q_2) \sigma_{ij} e^{ipx} (\partial_j A_i) u(q_1) \\
 &\stackrel{2.50}{=} \frac{e}{2m} \int d^3x \underbrace{\bar{u}(q_2) \varepsilon_{ijk} \sigma_k \partial_j (e^{ipx} A_i)}_{I_{2,1}} - \underbrace{\bar{u}(q_2) \varepsilon_{ijk} \sigma_k e^{ipx} (\partial_j A_i) u(q_1)}_{I_{2,2}}, \tag{2.49}
 \end{aligned}$$

where in the third line we used the following relation (proof in Appendix A.1) :

$$\sigma_{ij} = \varepsilon_{ijk} \sigma_k \mathbb{1}. \tag{2.50}$$

For $I_{2,1}$ we obtain:

$$\begin{aligned}
 I_{2,1} &= \frac{e}{2m} \int d^3x \bar{u}(q_2) \sigma^\rho \cdot (\nabla \times (e^{ipx} \mathbf{A})) u(q_1) \\
 &\stackrel{2.51}{=} \frac{e}{2m} \int d^3x \bar{u}(q_2) \nabla \cdot ((e^{ipx} \mathbf{A}) \times \boldsymbol{\sigma}) u(q_1) \\
 &= \frac{e}{2m} \int d\mathcal{S} \bar{u}(q_2) (e^{ipx} \mathbf{A}) \times \boldsymbol{\sigma} u(q_1)
 \end{aligned}$$

where the following identity was used with $\nabla \times \boldsymbol{\sigma} = 0$:

$$\nabla \cdot (\mathbf{A} \times \mathbf{B}) = \mathbf{B} \cdot (\nabla \times \mathbf{A}) - \mathbf{A} \cdot (\nabla \times \mathbf{B}). \tag{2.51}$$

Making the same assumption as for $I_{1,2}$, \mathbf{A} vanishes at infinity which causes this integral to be zero.

A separate treatment of $I_{2,2}$ results in

$$\begin{aligned}
 I_{2,2} &= \frac{-e}{2m} \int d^3x \bar{\psi}_2 (\sigma_k \varepsilon_{ijk} \partial_j A_i) \psi_1 \\
 &= \frac{e}{2m} \int d^3x \bar{\psi}_2 (\sigma_k \varepsilon_{kji} \partial_j A_i) \psi_1 \\
 &= \frac{e}{2m} \int d^3x \bar{\psi}_2^A (\sigma_k B_k) \psi_1^A \\
 &= \frac{e}{2m} \int d^3x \bar{\psi}_2^A (\boldsymbol{\sigma} \cdot \mathbf{B}) \psi_1^A \tag{2.52}
 \end{aligned}$$

Here we also applied the non-relativistic limit which eliminates the small components of ψ . Collecting all remaining terms merges in the final expression for the transition rate of:

$$T_{2,1} = -i2\pi \int d^3x \bar{\psi}_2^A \left(-e\varphi \mathbb{1} + \frac{e}{2m} \boldsymbol{\sigma} \cdot \mathbf{B} \right) \psi_1^A \tag{2.53}$$

In total, the direct comparison of Eq. 2.53 with the Hamiltonian in Eq. 2.31 shows that $g = 2$ follows also from the tree level diagram.

2.5 Electromagnetic Form Factors

This section is based on [13], P.315-318. The most general form of an interaction between a particle and an external electromagnetic field can be visualized by the following Feynman diagram where the central circle represents a placeholder for arbitrary loop-orders.

2 The Anomalous Magnetic Moment in the Standard Model

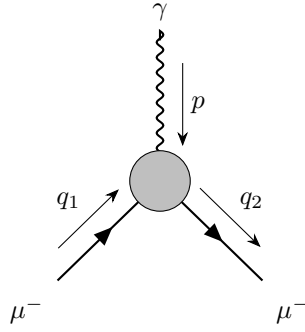


Figure 5: Generalized form of a Feynman diagram visualizing an electromagnetic interaction.

The generalized Feynman amplitude takes the form of

$$iM^\mu = \bar{u}(q_2)\Gamma^\mu u(q_1) \quad (2.54)$$

where Γ^μ is the vertex function and also acts as a placeholder for arbitrary loop levels. Γ^μ transforms like a four-vector and can be decomposed as a linear combination of all occurring Lorentz vectors. Hence, the vertex function can be expressed in its most general form as

$$iM^\mu = \bar{u}(q_2)(f_1\gamma^\mu + f_2p^\mu + f_3q_1^\mu + f_4q_2^\mu)u(q_1). \quad (2.55)$$

Hypothetically, this parameterization could also contain terms proportional to γ^5 . Those terms are especially taken into account in beyond QED theories. Due to the parity symmetry present in QED, these γ^5 terms do not contribute. Every possible occurrence of a Lorentz vector is weighted by the functions f_i . In general, they can also depend on products or contractions of different momenta namely \not{p} , q_1 , q_2 , p^2 , q_1^2 , q_2^2 , $p^\mu \cdot q_1^\mu$, $p^\mu \cdot q_2^\mu$, $q_1^\mu \cdot q_2^\mu$ and m . The set of possible dependencies can be reduced by employing the following considerations. The first constraint is momentum conservation which also holds for contractions with γ -matrices

$$p^\mu = q_2^\mu - q_1^\mu. \quad (2.56)$$

The dependency on the slashed momenta can be resolved by the application of the Dirac equation (Eq. 2.35), reducing the dependency purely on m . Furthermore, the muons are on their mass shells, which means that they fulfill the relativistic energy-mass relation:

$$q_{1,2}^2 = m^2. \quad (2.57)$$

The p^μ dependence can be resolved by inserting Eq. 2.56

$$iM^\mu = \bar{u}(q_2)(f_1\gamma^\mu + (f_3 - f_2)q_1^\mu + (f_4 + f_2)q_2^\mu)u(q_1) \quad (2.58)$$

which forces $f_2 = 0$ in order to match Eq. 2.55. For a further reduction, we can make use of the Ward-identity which states that

$$p_\mu M^\mu = 0. \quad (2.59)$$

Expanding gives us

$$\begin{aligned} 0 &= p_\mu \bar{u}(q_2)(f_1\gamma^\mu + f_3q_1^\mu + f_4q_2^\mu)u(q_1) \\ &= f_1 \bar{u}(q_2)\not{p}u(q_1) + f_3(p_\mu q_1^\mu)\bar{u}(q_2)u(q_1) + f_4(p_\mu q_2^\mu)\bar{u}(q_2)u(q_1) \\ &\stackrel{2.56}{=} f_1 \bar{u}(q_2)(q_2 - q_1)u(q_1) + f_3(p_\mu q_1^\mu)\bar{u}(q_2)u(q_1) + f_4(p_\mu q_2^\mu)\bar{u}(q_2)u(q_1) \\ &\stackrel{2.35}{=} f_3(p_\mu q_1^\mu)\bar{u}(q_2)u(q_1) + f_4(p_\mu q_2^\mu)\bar{u}(q_2)u(q_1) \\ &\stackrel{2.61}{=} f_3(p_\mu q_1^\mu)\bar{u}(q_2)u(q_1) - f_4(p_\mu q_1^\mu)\bar{u}(q_2)u(q_1) \\ f_3 &= f_4. \end{aligned} \quad (2.60)$$

2 The Anomalous Magnetic Moment in the Standard Model

In the fifth line we used

$$p_\mu q_1^\mu \stackrel{2.56}{=} q_2 \cdot q_1 - q_1^2 \stackrel{2.57}{=} q_2 \cdot q_1 - m^2 \stackrel{2.56}{=} q_2^2 - p \cdot q_2 - m^2 \stackrel{2.57}{=} -p \cdot q_2. \quad (2.61)$$

The yield of Eq. 2.60 is that only two independent factors f_1 and f_3 remain. The resulting invariant amplitude can be further expanded with the use of the Gordon identity.

$$\begin{aligned} iM^\mu &= \bar{u}(q_2)(f_1\gamma^\mu + f_3(q_1 + q_2))u \\ &\stackrel{A.13}{=} \bar{u}(q_2)(f_1\gamma^\mu + f_3(2m\gamma^\mu - i\sigma^{\mu\nu}(q_2 - q_1)_\nu))u \\ &\stackrel{2.56}{=} \bar{u}(q_2)((f_1 + 2mf_3)\gamma^\mu - f_3i\sigma^{\mu\nu}p_\nu)u(q_1) \end{aligned} \quad (2.62)$$

The prefactors are now accommodated in the form factors F_1 and F_2 defined as

$$F_1\left(\frac{p^2}{m^2}\right) = \frac{i}{e}(f_1 + 2mf_3) \quad \text{and} \quad F_2\left(\frac{p^2}{m^2}\right) = -\frac{i}{e}(2mf_3). \quad (2.63)$$

Inserting the form factors into Eq. 2.62 finalizes the structure of the invariant amplitude to

$$iM^\mu = (-ie)\bar{u}(q_2) \left[F_1(p^2)\gamma^\mu + F_2(p^2)\frac{i}{2m}\sigma^{\mu\nu}p_\nu \right] u(q_1). \quad (2.64)$$

For the considered scenario, m is fixed which reduces the dependency only to p^2 . The comparison of this expression with the tree-level diagram from Eq. 2.32 suggests the following choice for the form factors, since there was no occurrence of $\sigma^{\mu\nu}p_\nu$:

$$F_1 = 1 \quad \text{and} \quad F_2 = 0. \quad (2.65)$$

In the tree-level calculation, we showed that the Landé factor arising from this diagram satisfies precisely $g = 2$ (Eq. 2.53). This contribution is therefore covered by the form factor F_1 . In conclusion, any deviations from $g = 2$ will originate from F_2 . When considering the non-relativistic limit $p \rightarrow 0$, F_2 modifies the g -factor in the following way:

$$g = 2 + 2F_2(0). \quad (2.66)$$

The anomalous magnetic moment is for that reason defined as the deviation from $g = 2$

$$a_\mu = \frac{g - 2}{2} = F_2(0). \quad (2.67)$$

In the calculations at higher loop orders, the anomalous magnetic moment can therefore be identified as the coefficient of the operator $\sigma^{\mu\nu}p_\nu$ normalized by $\frac{2m}{e}$.

2.6 One-Loop QED Contribution

The goal is now to extract and identify the magnetic form factor $F_2(p^2)$ as a component of the invariant amplitude arising from the associated Feynman diagram. The calculation is retraced from [13], P.318-320.

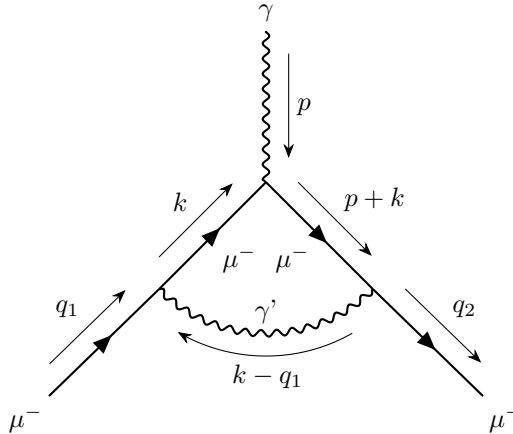


Figure 6: Topology of the one-loop QED diagram.

2 The Anomalous Magnetic Moment in the Standard Model

The application of the Feynman rules yields

$$iM^\mu = \int_{\mathbb{R}^4} \frac{d^4k}{(2\pi)^4} \bar{u}(q_2) \frac{-g^{\rho\nu}}{(k-q_1)^2 + i\varepsilon} (-ie\gamma^\rho) \frac{i(\not{p} + \not{k} + m)}{(p+k)^2 - m^2 + i\varepsilon} (-ie\gamma^\mu) \\ \times \frac{i(\not{k} + m)}{k^2 - m^2 + i\varepsilon} (-ie\gamma^\nu) u(q_1)$$

for the invariant amplitude, which can be simplified into

$$iM^\mu = -e^3 \bar{u}(q_2) \int_{\mathbb{R}^4} \frac{d^4k}{(2\pi)^4} \frac{\gamma_\nu(\not{p} + \not{k} + m)\gamma^\mu(\not{k} + m)\gamma^\nu}{[(k-q_1)^2 + i\varepsilon][(p+k)^2 - m^2 + i\varepsilon][k^2 - m^2 + i\varepsilon]} u(q_1) \quad (2.68)$$

Since all arbitrary virtual momenta k are possible, an integral over the four-dimensional momentum space is necessary. One can identify this integral to be of the form of

$$iM^\mu = -e^3 \int_{\mathbb{R}^4} \frac{d^4k}{(2\pi)^4} \frac{N^\mu}{ABC}, \quad (2.69)$$

where

$$N^\mu = \gamma_\nu(\not{p} + \not{k} + m)\gamma^\mu(\not{k} + m)\gamma^\nu \\ A = k^2 - m^2 + i\varepsilon \\ B = (p+k)^2 - m^2 + i\varepsilon \\ C = (k-q_1)^2 + i\varepsilon. \quad (2.70)$$

In order to decompose the integral, we make use of the Feynman parameterization that is discussed in Appendix A.4. For the case with three propagators in the denominator, it can be expanded via

$$\frac{1}{ABC} = 2 \int_0^1 dx dy dz \delta(x+y+z-1) \frac{1}{(Ax + By + Cz)^3}. \quad (2.71)$$

For x, y and z the relation

$$x + y + z = 1 \quad (2.72)$$

holds. In the following steps, the nominator and the denominator will be treated separately. We start with a simplification of the innermost part of the denominator

$$Ax + By + Cz = (k^2 - m^2 + i\varepsilon)x + ((p+k)^2 - m^2 + i\varepsilon)y + ((k-q_1)^2 + i\varepsilon)z \\ = (k^2 - m^2 + i\varepsilon)x + (p^2 + 2pk + k^2 - m^2 + i\varepsilon)y + (k^2 - 2kq_1 + q_1^2 + i\varepsilon)z \\ = (k^2 - m^2 + i\varepsilon)(1-y-z) + yp^2 + 2ypk + yk^2 - ym^2 + yi\varepsilon + zk^2 - 2zkq_1 + zq_1^2 + zi\varepsilon \\ = k^2 - m^2 + i\varepsilon - yk^2 + ym^2 - yi\varepsilon - zk^2 + zm^2 - zi\varepsilon \\ + yp^2 + 2ypk + yk^2 - ym^2 + yi\varepsilon + zk^2 - 2zkq_1 + zq_1^2 + zi\varepsilon \\ = k^2 - m^2 + i\varepsilon + zm^2 + yp^2 + 2ypk - 2zkq_1 + zq_1^2 \\ = k^2 - (1-z)m^2 + yp^2 + 2k(yp - zq_1) + zq_1^2 + i\varepsilon \equiv D. \quad (2.73)$$

In order to prepare an upcoming substitution, we will work out

$$(k^\mu + yp^\mu - zq_1^\mu)^2 = k^2 + 2k(yp - zq_1) + y^2p^2 - 2zypq_1 + z^2q_1^2 \\ \Leftrightarrow k^2 + 2k(yp - zq_1) = (k + yp - zq_1)^2 - y^2p^2 + 2zypq_1 - z^2q_1^2$$

so we can incorporate this new expression for the two terms in Eq. 2.73, resulting in

$$D = (k^\mu + yp^\mu - zq_1^\mu)^2 - \underbrace{y^2p^2 + 2zypq_1 - z^2q_1^2 + yp^2 + zq_1^2 - (1-z)m^2 + i\varepsilon}_{\equiv -\Delta} \quad (2.74)$$

2 The Anomalous Magnetic Moment in the Standard Model

We can now simplify Δ :

$$\begin{aligned}
\Delta &= y^2 p^2 - 2zypq_1 + z^2 q_1^2 - yp^2 - zq_1^2 + (1-z)m^2 \\
&= -(1-y)yp^2 - 2zypq_1 - z(1-z)q_1^2 + (1-z)m^2 \\
&= -(x+z)yp^2 - 2zypq_1 - z(1-z)m^2 + (1-z)m^2 \\
&= -xyp^2 - zyp^2 - 2zypq_1 + (1-z)^2 m^2 \\
&= -xyp^2 - yz(p^2 + 2pq_1 + q_1^2 - q_1^2) + (1-z)^2 m^2 \\
&= -xyp^2 - yz((p+q_1)^2 - q_1^2) + (1-z)^2 m^2 \\
&= -xyp^2 + (1-z)^2 m^2.
\end{aligned} \tag{2.75}$$

This leaves us with a compact version of the denominator

$$D = (k^\mu + yp^\mu - zq_1^\mu)^2 - \Delta + i\varepsilon \tag{2.76}$$

Introducing the substitution $k^\mu \rightarrow k^\mu - yp^\mu + zq_1^\mu$ yields

$$iM^\mu = -2e^3 \int_{\mathbb{R}^4} \frac{d^4 k}{(2\pi)^4} \int_0^1 dx dy dz \delta(x+y+z-1) \frac{N^\mu}{(k^2 - \Delta + i\varepsilon)^3} \tag{2.77}$$

for the amplitude. We will now further examine the numerator N^μ with the identities from Appendix A.1

$$N^\mu = \gamma_\nu (\not{p} + \not{k} + m) \gamma^\mu (\not{k} + m) \gamma^\nu \tag{2.78}$$

$$= \underbrace{\gamma_\nu \not{p} \gamma^\mu \not{k} \gamma^\nu}_1 + \underbrace{m \gamma_\nu \not{p} \gamma^\mu \gamma^\nu}_2 + \underbrace{\gamma_\nu \not{k} \gamma^\mu \not{k} \gamma^\nu}_3 + \underbrace{m \gamma_\nu \not{k} \gamma^\mu \gamma^\nu}_4 + \underbrace{m \gamma_\nu \gamma^\mu \not{k} \gamma^\nu}_5 + \underbrace{m^2 \gamma_\nu \gamma^\mu \gamma^\nu}_6. \tag{2.79}$$

We can simplify the individual terms in the following by working with the Dirac matrix identities. For term 1 and for term 3 analogously:

$$\gamma_\nu \gamma^\rho p_\rho \gamma^\mu \gamma^\sigma k_\sigma \gamma^\nu = p_\rho k_\sigma \gamma_\nu \gamma^\rho \gamma^\mu \gamma^\sigma \gamma^\nu \stackrel{A.9}{=} p_\rho k_\sigma (-2\gamma^\sigma \gamma^\mu \gamma^\rho) = -2\not{k} \gamma^\mu \not{p}. \tag{2.80}$$

For term 2,4 and 5:

$$m \gamma_\nu \gamma^\rho p_\rho \gamma^\mu \gamma^\nu = m p_\rho \gamma_\nu \gamma^\rho \gamma^\mu \gamma^\nu \stackrel{A.9}{=} 4m p_\rho g^{\rho\mu} = 4mp^\mu. \tag{2.81}$$

For term 6:

$$m^2 \gamma_\nu \gamma^\mu \gamma^\nu \stackrel{A.9}{=} -2m^2 \gamma^\mu. \tag{2.82}$$

Merging everything together results in

$$N^\mu = -2(\not{k} \gamma^\mu \not{p} + \not{k} \gamma^\mu \not{k} - 2m(p^\mu + 2k^\mu) + m^2 \gamma^\mu). \tag{2.83}$$

Applying the substitution $k^\mu \rightarrow k^\mu - yp^\mu + zq_1^\mu$ transforms this into

$$\begin{aligned}
-\frac{1}{2} N^\mu &= (\not{k} - y\not{p} + z\not{q}_1) \gamma^\mu \not{p} + (\not{k} - y\not{p} + z\not{q}_1) \gamma^\mu (\not{k} - y\not{p} + z\not{q}_1) - 2m(p^\mu + 2(k^\mu - yp^\mu + zq_1^\mu)) + m^2 \gamma^\mu \\
&= \cancel{\not{k} \gamma^\mu \not{p}} - y\not{p} \gamma^\mu \not{p} + z\not{q}_1 \gamma^\mu \not{p} + \not{k} \gamma^\mu \not{k} - \cancel{y\not{k} \gamma^\mu \not{p}} + \cancel{z\not{k} \gamma^\mu \not{q}_1} - \cancel{y\not{p} \gamma^\mu \not{k}} + y^2 \not{p} \gamma^\mu \not{p} - yz\not{p} \gamma^\mu \not{q}_1 \\
&\quad + \cancel{z\not{q}_1 \gamma^\mu \not{k}} - yz\not{q}_1 \gamma^\mu \not{p} + z^2 \not{q}_1 \gamma^\mu \not{q}_1 - 2mp^\mu - 4m\not{k}^\mu + 4myp^\mu - 4mzq_1^\mu + m^2 \gamma^\mu.
\end{aligned} \tag{2.84}$$

All terms that are linear in k or \not{k} vanish because of the symmetric integral bounds. The remaining terms give us

$$\begin{aligned}
-\frac{1}{2} N^\mu &= (-y\not{p} + z\not{q}_1) \gamma^\mu \not{p} + \not{k} \gamma^\mu \not{k} + \not{p} \gamma^\mu (y^2 \not{p} - yz\not{q}_1) - \not{q}_1 \gamma^\mu (zy\not{p} - z^2 \not{q}_1) \\
&\quad + 2m(2y-1)p^\mu - 4mzq_1^\mu + m^2 \gamma^\mu.
\end{aligned} \tag{2.85}$$

The next goal is to evaluate all contracted momenta. We can identify the following four types of combinations of γ -matrices which can be simplified. It is important to note that the vertex

2 The Anomalous Magnetic Moment in the Standard Model

function is still enclosed by the spinors $\bar{u}(q_2)$ and $u(q_1)$ and thus enables the application of the Dirac equation.

$$\begin{aligned}
1) \quad \not{p}\gamma^\mu\not{p} &= p_\nu p_\sigma \gamma^\nu \gamma^\mu \gamma^\sigma \stackrel{A.6}{=} p_\nu p_\sigma \gamma^\nu (2g^{\mu\sigma} - \gamma^\sigma \gamma^\mu) = 2\not{p}p^\mu - \not{p}\not{p}\gamma^\mu = 2(q_2 - q_1)p^\mu - p^2\gamma^\mu = -p^2\gamma^\mu \\
2) \quad \not{k}\gamma^\mu\not{k} &= k_\nu k_\sigma \gamma^\nu \gamma^\mu \gamma^\sigma \stackrel{2.88}{=} \frac{1}{4}k^2 g_{\nu\sigma} \gamma^\nu \gamma^\mu \gamma^\sigma = \frac{1}{4}k^2 \gamma^\nu \gamma^\mu \gamma_\nu \stackrel{A.9}{=} -\frac{1}{2}k^2 \gamma^\mu \\
3) \quad \gamma^\mu\not{p} &= \gamma^\mu(q_2 - q_1) = \gamma^\mu(q_2 - m) = \gamma^\mu \gamma^\nu q_{2\nu} - m\gamma^\mu \stackrel{A.6}{=} 2g^{\mu\nu} q_{2\nu} - q_2^\mu \gamma^\mu - m\gamma^\mu = 2(q_2^\mu - m\gamma^\mu) \\
4) \quad \not{p}\gamma^\mu &= (q_2 - q_1)\gamma^\mu = m\gamma^\mu - q_1^\mu \gamma^\mu = m\gamma^\mu - q_{1\nu} \gamma^\mu \gamma^\nu = m\gamma^\mu - 2q_1^\mu + \gamma^\mu q_1 = 2(m\gamma^\mu - q_1^\mu).
\end{aligned} \tag{2.86}$$

In the first calculation, we utilized that:

$$\not{p}\not{p} = p_\mu p_\nu \gamma^\mu \gamma^\nu \stackrel{A.6}{=} p_\mu p_\nu (2g^{\mu\nu} - \gamma^\nu \gamma^\mu) = 2p^2 - \not{p}\not{p}. \tag{2.87}$$

For the second calculation,

$$k^\mu k^\nu = \frac{1}{4}g^{\mu\nu} k^2 \tag{2.88}$$

was used. We can further examine the numerator Eq. 2.85 and want to sort everything the following way:

$$\begin{aligned}
-\frac{1}{2}N^\mu &= (-y\not{p} + zq_1)\gamma^\mu\not{p} + \not{k}\gamma^\mu\not{k} + \not{p}\gamma^\mu(y^2\not{p} - yzq_1) - q_1\gamma^\mu(zy\not{p} - z^2q_1) \\
&\quad + 2m(2y-1)p^\mu - 4mzq_1^\mu + m^2\gamma^\mu \\
&= -y\not{p}\gamma^\mu\not{p} + zq_1\gamma^\mu\not{p} + y^2\not{p}\gamma^\mu\not{p} - yz\not{p}\gamma^\mu q_1 - zyq_1\gamma^\mu\not{p} + z^2q_1\gamma^\mu q_1 \\
&\quad + \not{k}\gamma^\mu\not{k} + 2m(2y-1)p^\mu - 4mzq_1^\mu + m^2\gamma^\mu \\
&= (y^2 - y)\not{p}\gamma^\mu\not{p} + z(1-y)q_1\gamma^\mu\not{p} - yz\not{p}\gamma^\mu q_1 + z^2q_1\gamma^\mu q_1 \\
&\quad + \not{k}\gamma^\mu\not{k} + 2m(2y-1)p^\mu - 4mzq_1^\mu + m^2\gamma^\mu \\
&\stackrel{2.56}{=} (y^2 - y)\not{p}\gamma^\mu\not{p} + z(1-y)(q_2 - \not{p})\gamma^\mu\not{p} - yz\not{p}\gamma^\mu q_1 + z^2q_2\gamma^\mu q_1 - z^2\not{p}\gamma^\mu q_1 \\
&\quad + \not{k}\gamma^\mu\not{k} + 2m(2y-1)p^\mu - 4mzq_1^\mu + m^2\gamma^\mu \\
&\stackrel{2.35}{=} (y^2 - y - z(1-y))\not{p}\gamma^\mu\not{p} - z(y+z)m\not{p}\gamma^\mu + z(1-y)m\gamma^\mu\not{p} + z^2m^2\gamma^\mu \\
&\quad + \not{k}\gamma^\mu\not{k} + 2m(2y-1)p^\mu - 4mzq_1^\mu + m^2\gamma^\mu.
\end{aligned} \tag{2.89}$$

We can now insert the expressions from Eq. 2.86 which results in

$$\begin{aligned}
-\frac{1}{2}N^\mu &\stackrel{2.86}{=} -(y^2 - (y+z) + yz)p^2\gamma^\mu - 2z(y+z)m(m\gamma^\mu - q_1^\mu) + 2z(1-y)m(q_2^\mu - m\gamma^\mu) \\
&\quad - \frac{1}{2}k^2\gamma^\mu + 2m(2y-1)p^\mu - 4mzq_1^\mu + (1+z^2)m^2\gamma^\mu \\
&\stackrel{2.72}{=} \left(-\frac{1}{2}k^2 - (y^2 - (1-x) + y(1-x-y))p^2 - 2z(1-x)m^2 - 2z(1-y)m^2 + (1+z^2)m^2 \right) \gamma^\mu \\
&\quad + (2z(1-x)m - 4mz)q_1^\mu + 2z(1-y)mq_2^\mu + 2m(2y-1)p^\mu \\
&= \left(-\frac{1}{2}k^2 + (1-x)(1-y)p^2 + (-2z(1-x+1-y) + 1+z^2)m^2 \right) \gamma^\mu \\
&\quad + \underbrace{(2z(1-x)m - 4mz)q_1^\mu + 2z(1-y)mq_2^\mu + 2m(2y-1)p^\mu}_{\tilde{N}^\mu}.
\end{aligned} \tag{2.90}$$

From the underlined terms in Eq. 2.90 we want to construct a $q_1^\mu + q_2^\mu$ occurrence in order to apply

2 The Anomalous Magnetic Moment in the Standard Model

the Gordon identity. \tilde{N}^μ is rearranged to:

$$\begin{aligned}
\tilde{N}^\mu &= (2(1-x)zm - 4mz)q_1^\mu + 2zm(1-y)q_2^\mu - 2m(1-2y)p^\mu \\
&\stackrel{2.56}{=} (2(1-x)zm - 4zm + 2zm(1-y))q_2^\mu - (2(1-x)zm - 4zm + 2m(1-2y))p^\mu \\
&= -2zm(x+y)q_2^\mu - 2m((1-x)z - 2z + 1 - 2y)p^\mu \\
&\stackrel{2.72}{=} -mz(1-z)(q_2^\mu + q_2^\mu) - m(2(1-x)z - 4z + 2 - 4y)p^\mu \\
&\stackrel{2.56}{=} -mz(1-z)(q_2^\mu + q_1^\mu + p^\mu) - m(2(1-x)z - 4z + 2 - 4y)p^\mu \\
&= -mz(1-z)(q_2^\mu + q_1^\mu) + m(-2(1-x) + 4z - 2 + 4y - z(1-z))p^\mu \\
&= -mz(1-x)(q_1^\mu + q_2^\mu) + m(-2z + 2xz + 4z - 2 + 4y - z + z^2)p^\mu \\
&\stackrel{2.72}{=} -mz(1-x)(q_1^\mu + q_2^\mu) + m(2(1-x-y) + 2xz - 2 + 4y - z + z(1-x-y))p^\mu \\
&= -mz(1-x)(q_1^\mu + q_2^\mu) + m(xz - 2x + 2y - yz)p^\mu \\
&= -mz(1-x)(q_1^\mu + q_2^\mu) + m(z-2)(x-y)p^\mu. \tag{2.91}
\end{aligned}$$

Now the Gordon identity (Appendix A.13) can be used to replace $q_1^\mu + q_2^\mu$ in the total numerator:

$$\begin{aligned}
-\frac{1}{2}N^\mu &= \left(-\frac{1}{2}k^2 + (1-x)(1-y)p^2 + (-2z(2-x-y) + 1 + z^2)m^2 \right) \gamma^\mu \\
&\quad - mz(1-z)(q_1^\mu + q_2^\mu) + m(z-2)(x-y)p^\mu \\
&\stackrel{A.13}{=} \left(-\frac{1}{2}k^2 + (1-x)(1-y)p^2 + (-2z(2-x-y) + 1 + z^2)m^2 \right) \gamma^\mu \\
&\quad - mz(1-z)(2m\gamma^\mu - i\sigma^{\mu\nu}p_\nu) + m(z-2)(x-y)p^\mu \\
&= \left(-\frac{1}{2}k^2 + (1-x)(1-y)p^2 + (-2z(2-x-y) + 1 + z^2 - 2z(1-z))m^2 \right) \gamma^\mu \\
&\quad + imz(1-z)\sigma^{\mu\nu}p_\nu + m(z-2)(x-y)p^\mu \\
&\stackrel{2.72}{=} \left(-\frac{1}{2}k^2 + (1-x)(1-y)p^2 + (-2z(1+z) + 1 + z^2 - 2z(1-z))m^2 \right) \gamma^\mu \\
&\quad + imz(1-z)\sigma^{\mu\nu}p_\nu + m(z-2)(x-y)p^\mu \\
&= \left(-\frac{1}{2}k^2 + (1-x)(1-y)p^2 + (-2z - 2z^2 + 1 + z^2 - 2z + 2z^2)m^2 \right) \gamma^\mu \\
&\quad + imz(1-z)\sigma^{\mu\nu}p_\nu + m(z-2)(x-y)p^\mu \\
&= \left(-\frac{1}{2}k^2 + (1-x)(1-y)p^2 + (1 - 4z + z^2)m^2 \right) \gamma^\mu \\
&\quad + imz(1-z)\sigma^{\mu\nu}p_\nu + m(z-2)(x-y)p^\mu. \tag{2.92}
\end{aligned}$$

The reduction of the numerator to this compact form allows us to extract the magnetic contribution via the magnetic formfactor $F_2(p^2)$, which accommodates everything that is proportional to $\sigma^{\mu\nu}p_\nu$. The relevant part of the numerator labeled as N_m^μ then becomes

$$N_m^\mu = -2imz(1-z)\sigma^{\mu\nu}p_\nu. \tag{2.93}$$

Recalling from Eq. 2.64 that the formfactor $F_2(p^2)$ was defined as the coefficient of $p_\nu \bar{u}(q_2)\sigma^{\mu\nu}u(q_1)$ normalized by a factor of $2m/e$ yields the following expression for the formfactor:

$$F_2(p^2) = \frac{2m}{e} \left(4ie^3m \int_0^1 dx dy dz \delta(x+y+z-1) \int_{\mathbb{R}^4} d^4k \frac{z(1-z)}{(k^2 - \Delta + i\varepsilon)^3} \right). \tag{2.94}$$

Utilizing

$$\int_{\mathbb{R}^4} d^4k \frac{1}{(k^2 - \Delta + i\varepsilon)^3} = \frac{-i}{32\pi^2\Delta} \tag{2.95}$$

(proven in Appendix A.5) simplifies the formfactor with the denominator from Eq. 2.75 to

$$F_2(p^2) = \frac{8m^2e^2}{32\pi^2} \int_0^1 dx dy dz \delta(x+y+z-1) \frac{z(1-z)}{-xy p^2 + (1-z)^2 m^2}. \tag{2.96}$$

3 Electroweak One-Loop Contributions for Scalar-Fermion Interactions

In the non-relativistic limit of $p^2 \rightarrow 0$ this aggregates in

$$F_2(0) = \frac{8e^2}{32\pi^2} \int_0^1 dx dy dz \delta(x+y+z-1) \frac{z}{(1-z)}. \quad (2.97)$$

Performing the integration finalizes the calculation under the introduction of the fine-structure constant $\alpha = e^2/4\pi$

$$\begin{aligned} F_2(0) &= \frac{\alpha}{\pi} = \int_0^1 dz \int_0^{1-z} dy \frac{z}{1-z} \\ &= \frac{\alpha}{\pi} \int_0^1 dz \left(\frac{zy}{1-z} \Big|_0^{1-z} \right) = \frac{\alpha}{\pi} \int_0^1 dz z \end{aligned} \quad (2.98)$$

into the result of

$$\boxed{F_2(0) = \frac{\alpha}{2\pi}} \quad (2.99)$$

which is the one-loop contribution to the anomalous magnetic moment of the muon. This result was first calculated by Julian Schwinger in 1948 [6]. Together with Eq. 2.66 we obtain the numerical value of:

$$a_\mu = \frac{\alpha}{2\pi} \approx 0.00116 \quad \text{and} \quad g = \left(2 + \frac{\alpha}{\pi}\right) \approx 2.00232. \quad (2.100)$$

One can notice that this result is independent of the fermion mass and is therefore the same for all leptons. For the current theoretical value of $a_\mu(\text{SM})$ [3], QED diagrams up to the fifth loop order $\mathcal{O}(\alpha^5)$ have been numerically evaluated, making it the most precise calculated quantity in particle physics. Besides the QED diagrams, there are also contributions from electroweak and hadronic loop diagrams. The hadronic contributions are the biggest source of uncertainty, since non-perturbative methods from lattice QCD have to be used.

3 Electroweak One-Loop Contributions for Scalar-Fermion Interactions

The discrepancy between the theoretical and experimental value of a_μ raises the assumption that there are missing contributions within the SM prediction. For that reason, a general approach of describing one-loop electroweak interactions of fermions and scalars is presented, which can then be adjusted for possible beyond Standard Model (BSM) models.

3.1 The Anomalous Magnetic Moment in Arbitrary Scalar-Fermion Interaction Models

The goal is now to obtain general formulae for the relevant contribution to the AMM arising from electroweak interactions. As a preparation for the upcoming calculation, the interaction vertices between scalars and fermions have to be analyzed with the aim to extract the associated Feynman rules. Interactions between scalars and fermions are in general mediated by Yukawa interactions. The Yukawa interaction Lagrangian [14] is given by as:

$$\begin{aligned} \mathcal{L}_{\text{Yukawa}} &= \sum_{F,H} \overline{\mu}^- (c_s + c_p \gamma^5) FH + \text{h.c.} \\ &= \sum_{F,H} \overline{\mu}^- (c_s + c_p \gamma^5) FH + H^* \cdot \bar{F} (c_s^* - c_p^* \gamma^5) \mu^- \end{aligned} \quad (3.1)$$

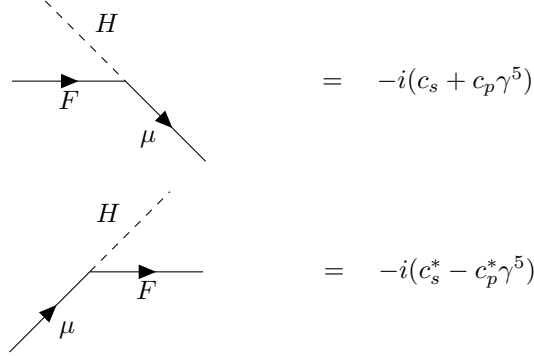
where μ , F , and H are the gauge fields and c_s and c_p are the model dependent scalar and pseudoscalar complex coupling constants. The summation is performed over all fermions and Higgs

3 Electroweak One-Loop Contributions for Scalar-Fermion Interactions

scalars of the corresponding model. The relative minus sign is the result of the anti-commutative nature of the γ^5 matrix (Eq. A.11):

$$\begin{aligned} \left(\overline{\mu^-}(c_s + c_p\gamma^5)FH\right)^\dagger &= \left(H^*F^\dagger(c_s^* + c_p^*\gamma^5) \cdot \overline{\mu^-}^\dagger\right) \\ &= \left(H^*F^\dagger(c_s^* + c_p^*\gamma^5) \cdot \gamma^0\mu^-\right) \\ &\stackrel{A.11}{=} \left(H^*\overline{F}(c_s^* - c_p^*\gamma^5) \cdot \mu^-\right). \end{aligned} \quad (3.2)$$

From this Lagrangian, the vertex rules can be read off by removing the fields and including a factor of $-i$:



3.2 Photon Absorption from the Internal Scalar Line

The first scenario under investigation is depicted in the Feynman-diagram in Fig. 7. The incoming muon splits up into virtual fermion F and a virtual scalar H . The scalar then interacts with the photon from the electromagnetic field. For this interaction, the scalar has to be at least singly charged.

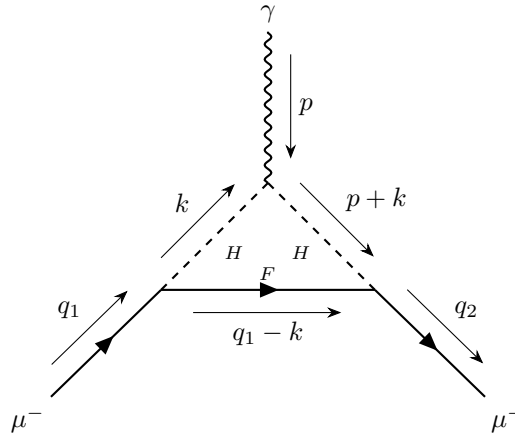


Figure 7: Topology of the electroweak one-loop diagram with an electromagnetic interaction mediated from a scalar.

The application of the Feynman-rules from Appendix A.2 leads to the following form of the invariant amplitude:

$$\begin{aligned} iM^\mu &= \int_{\mathbb{R}^4} \frac{d^4k}{(2\pi)^4} \bar{u}(q_2) (-i(c_s + c_p\gamma^5)) \frac{i(q_1 - \not{k} + m_F)}{(q_1 - k)^2 - m_F^2 + i\varepsilon} \frac{i}{(p+k)^2 - m_H^2 + i\varepsilon} (-iq_H e(2k+p)) \\ &\quad \times \frac{i}{k^2 - m_H^2 + i\varepsilon} (-i(c_s^* - c_p^*\gamma^5)) u(q_1). \end{aligned}$$

3 Electroweak One-Loop Contributions for Scalar-Fermion Interactions

This can be simplified into

$$iM^\mu = q_H \cdot e \int_{\mathbb{R}^4} \frac{d^4k}{(2\pi)^4} \bar{u}(q_2) \frac{(c_s + c_p \gamma^5)(q_1 - \not{k} + m_F)(2k + p)(c_s^* - c_p^* \gamma^5)}{((q_1 - k)^2 - m_F^2 + i\varepsilon)((p + k)^2 - m_H^2 + i\varepsilon)(k^2 - m_H^2 + i\varepsilon)} u(q_1). \quad (3.3)$$

Just as for the QED calculation one can identify the following structure of the integral:

$$iM^\mu = q_H \cdot e \int_{\mathbb{R}^4} \frac{d^4k}{(2\pi)^4} \frac{N^\mu}{ABC} \quad (3.4)$$

where

$$\begin{aligned} N^\mu &= (c_s + c_p \gamma^5)(q_1 - \not{k} + m_F)(2k + p)(c_s^* - c_p^* \gamma^5) \\ A &= k^2 - m_H^2 + i\varepsilon \\ B &= (p + k)^2 - m_H^2 + i\varepsilon \\ C &= (q_1 - k)^2 - m_F^2 + i\varepsilon. \end{aligned} \quad (3.5)$$

In order to decompose this integral, the Feynman parameterization is introduced. In the case of $n = 3$ factors in the denominator, it can be expanded via

$$\frac{1}{ABC} = 2 \int_0^1 dx dy dz \delta(x + y + z - 1) \frac{1}{(Ax + By + Cz)^3} \quad (3.6)$$

In the following steps, the nominator and the denominator will be treated separately. We start with a simplification of the innermost part of the denominator.

$$\begin{aligned} Ax + By + Cz &= x(k^2 - m_H^2 + i\varepsilon) + y((p + k)^2 - m_H^2 + i\varepsilon) + z((q_1 - k)^2 - m_F^2 + i\varepsilon) \\ &= (1 - y - z)(k^2 - m_H^2 + i\varepsilon) + y(p^2 + 2pk + k^2 - m_H^2 + i\varepsilon) + z(q_1^2 - 2q_1k + k^2 - m_F^2 + i\varepsilon) \\ &= k^2 - (1 - z)m_H^2 + yp^2 + 2ypk + zq_1^2 - 2zq_1k - zm_F^2 + i\varepsilon \\ &= k^2 - (1 - z)m_H^2 + yp^2 + 2k(yp - zq_1) + zq_1^2 - zm_F^2 + i\varepsilon \end{aligned} \quad (3.7)$$

In order to prepare the k substitution we expand

$$\begin{aligned} (k^\mu + yp^\mu - zq_1^\mu)^2 &= k^2 + 2k(yp - zq_1) + y^2p^2 - 2zypq_1 + z^2q_1^2 \\ \Leftrightarrow k^2 + 2k(yp - zq_1) &= (k + yp - zq_1)^2 - y^2p^2 + 2zypq_1 - z^2q_1^2 \end{aligned} \quad (3.8)$$

so that the denominator D becomes

$$D = (k + yp - zq_1)^2 \underbrace{-y^2p^2 + 2zypq_1 - z^2q_1^2 - (1 - z)m_H^2 + yp^2 + zq_1^2 - zm_F^2 + i\varepsilon}_{\equiv -\Delta'}. \quad (3.9)$$

The auxiliary variable Δ' is used to store all non k -dependent terms

$$\begin{aligned} \Delta' &= y^2p^2 - 2zypq_1 + z^2q_1^2 + (1 - z)m_H^2 - yp^2 - zq_1^2 + zm_F^2 \\ &= -y(1 - y)p^2 - 2zypq_1 - z(1 - z)q_1^2 + (1 - z)m_H^2 + zm_F^2 \\ &= -y(x + z)p^2 - 2zypq_1 - z(x + y)q_1^2 + (1 - z)m_H^2 + zm_F^2 \\ &= -xyp^2 - yzp^2 - 2zypq_1 - zxq_1^2 - zyq_1^2 + (1 - z)m_H^2 + zm_F^2 \\ &= -xyp^2 - yz(p + q_1)^2 - zxq_1^2 + (1 - z)m_H^2 + zm_F^2 \\ &= -xyp^2 - yzq_2^2 - zxq_1^2 + (1 - z)m_H^2 + zm_F^2 \\ &= -xyp^2 - z(x + y)m_\mu^2 + (1 - z)m_H^2 + zm_F^2 \\ &= -xyp^2 - z(1 - z)m_\mu^2 + (1 - z)m_H^2 + zm_F^2 \\ &= -xyp^2 + m_\mu^2 z^2 + m_H^2(1 - z) + (m_F^2 - m_\mu^2)z. \end{aligned} \quad (3.10)$$

The denominator can now be expressed as

$$D = (k^\mu + yp^\mu - zq_1^\mu)^2 - \Delta' + i\varepsilon \quad (3.11)$$

3 Electroweak One-Loop Contributions for Scalar-Fermion Interactions

where the substitution $k^\mu \rightarrow k^\mu - yp^\mu + zq_1^\mu$ yields

$$D = k^2 - \Delta' + i\varepsilon. \quad (3.12)$$

We can now examine the numerator

$$N^\mu = \bar{u}(q_2)(c_s + c_p\gamma^5) \underbrace{(q_1 - \not{k} + m_F)(2k + p)(c_s^* - c_p^*\gamma^5)u(q_1)}_{\equiv \zeta^\mu}. \quad (3.13)$$

The innermost part defined as ζ^μ will be evaluated by starting off with the substitution $k^\mu \rightarrow k^\mu - yp^\mu + zq_1^\mu$:

$$\begin{aligned} \zeta^\mu &= 2q_1 k + q_1 p - 2\not{k}k - \not{k}p + 2m_F k^\mu + m_F p^\mu \\ &\stackrel{\text{sub}}{=} 2q_1(k^\mu - yp^\mu + zq_1^\mu) + q_1 p - 2(\not{k} - y\not{p} + zq_1)(k^\mu - yp^\mu + zq_1^\mu) - (\not{k} - y\not{p} + zq_1)p^\mu \\ &\quad + 2m_F(k^\mu - yp^\mu + zq_1^\mu) + m_F p^\mu \\ &\stackrel{\text{lin}}{=} \cancel{2q_1 k^\mu} - 2yq_1 p^\mu + 2zq_1 q_1^\mu + q_1 p^\mu - 2\not{k}k^\mu + 2y\not{k}p^\mu - \cancel{2z\not{k}q_1^\mu} + \cancel{2y\not{p}k^\mu} - 2y^2\not{p}p^\mu + 2yz\not{p}q_1^\mu \\ &\quad - \cancel{2zq_1 k^\mu} + 2yzq_1 p^\mu - 2z^2q_1 q_1^\mu - \cancel{\not{k}p^\mu} + y\not{p}p^\mu - zq_1 p^\mu + \cancel{2m_F k^\mu} - 2m_F y p^\mu + 2m_F z q_1^\mu + m_F p^\mu \\ &= -2\not{k}k^\mu + (-2yp^\mu + 2zq_1^\mu + p^\mu + 2yzp^\mu - 2z^2q_1^\mu - zp^\mu)q_1 + (-2y^2p^\mu + 2yzq_1^\mu + yp^\mu)\not{p} \\ &\quad + (-2yp^\mu + 2zq_1^\mu + p^\mu)m_F \\ &= -2\not{k}k + (2z(1-z)q_1^\mu + (1-z)p^\mu + 2yzp^\mu - 2yp^\mu)q_1 + (-y(2y-1)p^\mu + 2yzq_1^\mu)(q_2 - q_1) \\ &\quad + m_F(2zq_1^\mu - (2y-1)p^\mu) \\ &= -\frac{1}{2}k^2\gamma^\mu + ((2zq_1^\mu + p^\mu)(1-z) - 2y(1-z)p^\mu + y(2y-1)p^\mu - 2yzq_1^\mu)q_1 \\ &\quad + y(2zq_1^\mu - (2y-1)p^\mu)q_2 + (2zq_1^\mu - (2y-1)p^\mu)m_F \\ &\stackrel{2.72}{=} -\frac{1}{2}k^2\gamma^\mu + (2zq_1^\mu + p^\mu)(x+y) - 2(x+y) + y(2y-1)p^\mu - 2yzq_1^\mu)q_1 \\ &\quad + y(2zq_1^\mu - (2y-1)p^\mu)q_2 + (2zq_1^\mu - (2y-1)p^\mu)m_F \\ &= -\frac{1}{2}k^2\gamma^\mu + x(2zq_1^\mu - (2y-1)p^\mu)q_1 + y(2zq_1^\mu - (2y-1)p^\mu)q_2 + (2zq_1^\mu - (2y-1)p^\mu)m_F \\ &= -\frac{1}{2}k^2\gamma^\mu + (2zq_1^\mu - (2y-1)p^\mu)(xq_1 + yq_2 + m_F). \end{aligned} \quad (3.14)$$

Reconstructing N^μ yields

$$N^\mu = (c_s + c_p\gamma^5)\left(-\frac{1}{2}k^2\gamma^\mu + (2zq_1^\mu - (2y-1)p^\mu)(xq_1 + yq_2 + m_F)(c_s^* - c_p^*\gamma^5)\right). \quad (3.15)$$

In order to apply the Dirac equation we have to commute $c_s^* + c_p^*\gamma^5$. Since the γ^5 matrix anticommutes with all other γ matrices, we will get a relative minus sign from the commutation with q_1 and q_2

$$\begin{aligned} N^\mu &= (c_s + c_p\gamma^5)\underbrace{\left(c_s^*\left(-\frac{1}{2}k^2\gamma^\mu + (2zq_1^\mu - (2y-1)p^\mu)(xq_1 + yq_2 + m_F)\right)\right)}_{\equiv \zeta_+^\mu} \\ &\quad + c_p^*\gamma^5\underbrace{\left(-\frac{1}{2}k^2\gamma^\mu + (2zq_1^\mu - (2y-1)p^\mu)(xq_1 + yq_2 - m_F)\right)}_{\equiv \zeta_-^\mu} \\ &= |c_s|^2\zeta_+^\mu + |c_p|^2\zeta_-^\mu + \gamma^5(c_s c_p^*\zeta_-^\mu + c_s^* c_p \zeta_+^\mu). \end{aligned} \quad (3.16)$$

We can now apply the Dirac equation to transform q_1 and q_2 both into m_μ such that

$$\zeta_\pm^\mu = -\frac{1}{2}k^2\gamma^\mu + (2zq_1^\mu - (2y-1)p^\mu)((1-z)m_\mu \pm m_F) \quad (3.17)$$

3 Electroweak One-Loop Contributions for Scalar-Fermion Interactions

where Eq. 2.72 is used again. Now we incorporate $2q_1 = q_1 + q_2 - p$ resulting in

$$\begin{aligned}\zeta_{\pm}^{\mu} &= -\frac{1}{2}k^2\gamma^{\mu} + (z(q_1^{\mu} + q_2^{\mu}) - (z - (2y - 1))p^{\mu})((1 - z)m_{\mu} \pm m_F) \\ &\stackrel{A.13}{=} -\frac{1}{2}k^2\gamma^{\mu} + (z(2m\gamma^{\mu} - i\sigma^{\mu\nu}p_{\nu}) - (z - (2y - 1))p) ((1 - z)m_{\mu} \pm m_F).\end{aligned}\quad (3.18)$$

Since only the terms proportional to $\sigma^{\mu\nu}p_{\nu}$ contribute a to the AMM all other terms are neglected such that

$$\zeta_{\pm}^{\mu} = -iz((1 - z)m_{\mu} \pm m_F)\sigma^{\mu\nu}p_{\nu}.\quad (3.19)$$

By examining the structure of Eq. 3.16 it becomes evident that only the terms proportional to $|c_s|^2$ and $|c_p|^2$ contribute, since the crossing terms are multiplied with γ^5 . N^{μ} takes now the form of

$$N^{\mu} = \underbrace{(-iz)(|c_s|^2((1 - z)m_{\mu} + m_F) + |c_p|^2((1 - z)m_{\mu} - m_F))}_{\frac{e}{2m}F_2(p^2)}\sigma^{\mu\nu}p_{\nu}\quad (3.20)$$

where we identify the formfactor $F_2(p^2)$. Bringing together the expressions for the nominator and the denominator gives us

$$\begin{aligned}F_2(p^2) &= -q_H e \cdot \frac{2m}{e} \cdot 2 \int_{\mathbb{R}^4} \frac{d^4k}{(2\pi)^4} \int_0^1 dx dy dz \delta(x + y + z - 1) \\ &\quad \times \frac{iz|c_s|^2((1 - z)m_{\mu} + m_F) + |c_p|^2((1 - z)m_{\mu} - m_F)}{(k^2 - \Delta' + i\varepsilon)^3}.\end{aligned}\quad (3.21)$$

The numerator is independent of k . This enables us to evaluate the k integration immediately using again (Appendix A.5)

$$\int_{\mathbb{R}^4} \frac{d^4k}{(2\pi)^4} \frac{1}{(k^2 - \Delta' + i\varepsilon)^3} = \frac{-i}{32\pi^2\Delta'}.\quad (3.22)$$

This leads to

$$\begin{aligned}F_2(p^2) &= -\frac{q_H m_{\mu}^2}{8\pi^2} \int_0^1 dx dy dz \delta(x + y + z - 1) \\ &\quad \times \frac{|c_s|^2(z(1 - z) + \frac{m_F}{m_{\mu}}) + |c_p|^2(z(1 - z) - \frac{m_F}{m_{\mu}})}{-xyp^2 + m_{\mu}^2 z^2 + m_H^2(1 - z) + (m_F^2 - m_{\mu}^2)z}.\end{aligned}\quad (3.23)$$

Applying the non-relativistic limit ($p^2 \rightarrow 0$) and performing the x -integration yields

$$\begin{aligned}F_2(0) &= -\frac{q_H m_{\mu}^2}{8\pi^2} \int_0^1 dz \int_0^{1-z} dy \\ &\quad \times \frac{|c_s|^2(z(1 - z) + \frac{m_F}{m_{\mu}}) + |c_p|^2(z(1 - z) - \frac{m_F}{m_{\mu}})}{m_{\mu}^2 z^2 + m_H^2(1 - z) + (m_F^2 - m_{\mu}^2)z}.\end{aligned}\quad (3.24)$$

We can now evaluate the y -Integration:

$$F_2(0) = -\frac{q_H m_{\mu}^2}{8\pi^2} \int_0^1 dz \frac{(|c_s|^2(z(1 - z) + \frac{m_F}{m_{\mu}}) + |c_p|^2(z(1 - z) - \frac{m_F}{m_{\mu}}))(1 - z)}{m_{\mu}^2 z^2 + m_H^2(1 - z) + (m_F^2 - m_{\mu}^2)z}.\quad (3.25)$$

In the final step we apply the substitution $z' = 1 - z$:

$$F_2(0) = -\frac{q_H m_{\mu}^2}{8\pi^2} \int_0^1 dz' \frac{(|c_s|^2((z' - 1)(z') + \frac{m_F}{m_{\mu}}) + |c_p|^2((z' - 1)(z') - \frac{m_F}{m_{\mu}}))(z')}{m_{\mu}^2(1 - z')^2 + m_H^2 z' + (m_F^2 - m_{\mu}^2)(1 - z')}.\quad (3.26)$$

Expanding the terms gives us the final expression for the electroweak one-loop contribution to the AMM.

$$\boxed{a_{\mu}^s = -\frac{q_H m_{\mu}^2}{8\pi^2} \int_0^1 dz' \frac{|c_s|^2(z'^3 - z'^2 + \frac{m_F}{m_{\mu}}(z'^2 - z')) + |c_p|^2(z'^3 - z'^2 - \frac{m_F}{m_{\mu}}(z'^2 - z'))}{m_{\mu}^2 z'^2 + m_F^2(1 - z') + (m_H^2 - m_{\mu}^2)z'}}\quad (3.27)$$

which is in accordance with the expression for $[a_{\mu}]_c$ in [14] and was also cross-checked with the extension *package-X* [7] in *Mathematica* (Appendix A.6).

3.3 Photon Absorption from the Internal Fermion Line

In this topology, the internal charged fermion interacts with a photon of the electromagnetic field.

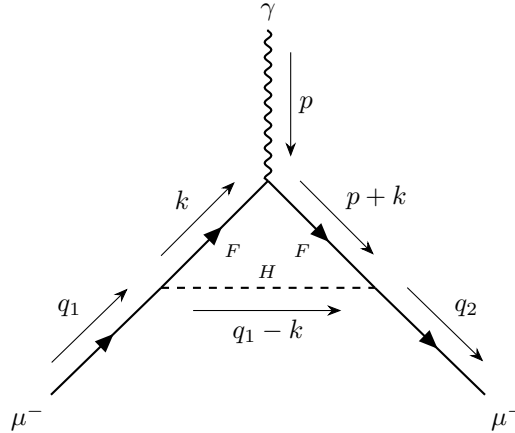


Figure 8: Topology of the Feynman diagram corresponding to the absorption of a photon via the internal fermion line.

The application of the Feynman rules results in the following invariant amplitude:

$$iM^\mu = \int_{\mathbb{R}^4} \frac{d^4k}{(2\pi)^4} \bar{u}(q_2) (-i(c_s + c_p \gamma^5)) \frac{i}{(q_1 - k)^2 - m_H^2 + i\varepsilon} \frac{i(\not{p} + \not{k} + m_F)}{(p+k)^2 - m_F^2 + i\varepsilon} \times (iq_F e \gamma^\mu) \frac{i(\not{k} + m_F)}{k^2 - m_F^2 + i\varepsilon} (-i(c_s^* - c_p^* \gamma^5)) u(q_1) \quad (3.28)$$

which can be simplified to

$$iM^\mu = -q_F e \int_{\mathbb{R}^4} \frac{d^4k}{(2\pi)^4} \bar{u}(q_2) \frac{(c_s + c_p \gamma^5)(\not{p} + \not{k} + m_F) \gamma^\mu (\not{k} + m_F)(c_s^* - c_p^* \gamma^5)}{((p+k)^2 - m_F^2 + i\varepsilon)((q_1 - k)^2 - m_H^2 + i\varepsilon)(k^2 - m_F^2 + i\varepsilon)} \quad (3.29)$$

The contribution to the AMM is given as

$$F_2^F(q^2) = -\frac{q_F m_\mu^2}{8\pi^2} \int_0^1 dz' \frac{|c_s|^2 (-z'^3 + z'^2 + \frac{m_F}{m_\mu} z'^2) + |c_p|^2 (-z'^3 + z'^2 - \frac{m_F}{m_\mu} z'^2)}{m_\mu^2 z'^2 + m_H^2 (1 - z') + (m_F^2 - m_\mu^2) z'} \quad (3.30)$$

This result can also be reproduced with *package-X* [7] in *Mathematica* (see. Appendix A.6).

4 The Two-Higgs-Doublet Model

The 2HDM extends the scalar sector of the SM and is mostly motivated by the concept of supersymmetry [15]. The 2HDM provides a rich phenomenology enabling the explanation of various unsolved phenomena in the Standard Model eg. dark matter and neutrino mass [16], the baryogenesis [17] and -out of particular interest for this work- the muon $g - 2$ anomaly. In the following section, the muon ($g - 2$) anomaly is resolved within the 2HDM, resulting in constraints on the properties of the new BSM particles in question. The following description of the 2HDM is based on [5],[18],[19].

4.1 Introduction to the Two-Higgs-Doublet Model

The 2HDM proposes the existence of a second SU(2) Higgs doublet Φ_2 alongside the SM doublet Φ_1 , each carrying hypercharge of $Y = 1/2$:

$$\Phi_i = \begin{pmatrix} \phi_i^+ \\ \frac{1}{\sqrt{2}}(v_i + \rho_i + i\eta_i) \end{pmatrix} \quad i = 1, 2 \quad (4.1)$$

4 The Two-Higgs-Doublet Model

Both doublets acquire vacuum expectation values (VEV) of $\langle \Phi_i \rangle = v_i/\sqrt{2}$. Complying with the conservation of the hypercharge, it turns out to be convenient to represent the doublets in a rotated basis given as

$$\begin{pmatrix} H_1 \\ H_2 \end{pmatrix} = \begin{pmatrix} \cos \beta & \sin \beta \\ -\sin \beta & \cos \beta \end{pmatrix} \begin{pmatrix} \Phi_1 \\ \Phi_2 \end{pmatrix}. \quad (4.2)$$

Here, β is defined as $\beta = \arctan(v_2/v_1)$ where v_i is the VEV of the corresponding doublet. In this specific basis, only the H_1 doublet acquires a non-vanishing VEV:

$$\langle H_1 \rangle = \frac{v}{\sqrt{2}} \quad \text{and} \quad \langle H_2 \rangle = 0. \quad (4.3)$$

The rotated doublets can be parameterized as:

$$H_1 = \begin{pmatrix} G^+ \\ \frac{1}{\sqrt{2}}(v + H_1^0 + iG^0) \end{pmatrix}, \quad H_2 = \begin{pmatrix} H^+ \\ \frac{1}{\sqrt{2}}(H_2^0 + iA^0) \end{pmatrix}. \quad (4.4)$$

In this form, G^+ and G^0 are the Goldstone Bosons, that get eaten up by the W - and Z -Bosons in the process of electroweak symmetry breaking. The remaining particles are two neutral CP-even scalars $H_{1,2}^0$, a CP-odd scalar A and a charged scalar H^+ . The VEV is now given as $v = \sqrt{v_1^2 + v_2^2} \approx 246$ GeV. The potential in the rotated basis takes the form of:

$$\begin{aligned} V = & m_{11}^2 H_1^\dagger H_1 + m_{22}^2 H_2^\dagger H_2 - \{m_{12}^2 (H_1^\dagger H_2 + H_2^\dagger H_1)\} \\ & + \frac{\lambda_1}{2} (H_1^\dagger H_1)^2 + \frac{\lambda_2}{2} (H_2^\dagger H_2)^2 + \lambda_3 (H_1^\dagger H_1)(H_2^\dagger H_2) \\ & + \lambda_4 (H_1^\dagger H_2)(H_2^\dagger H_1) + \frac{\lambda_5}{2} (H_1^\dagger H_2)^2 + \frac{\lambda_5^*}{2} (H_2^\dagger H_1)^2 \\ & + \lambda_6 (H_1^\dagger H_1)(H_1^\dagger H_2) + \lambda_6^* (H_2^\dagger H_1)(H_1^\dagger H_1) \\ & + \lambda_7 (H_2^\dagger H_2)(H_1^\dagger H_2) + \lambda_7^* (H_2^\dagger H_1)(H_2^\dagger H_2) \end{aligned} \quad (4.5)$$

where m_{12}^2 and $\lambda_{5,6,7}$ can be complex in general and the rest of the parameters are real. The masses of these particles can be obtained by finding the eigenvalues to the mass eigenstates of the squared mass matrix given as:

$$M_{ij}^2 = \frac{\partial^2 V}{\partial \phi_i^\dagger \partial \phi_j} \quad (4.6)$$

where ϕ_i is the corresponding particle. The explicit calculation of the diagonal elements can be found in Appendix A.7. The mass matrix for the charged scalars is already diagonalized. For the neutral scalars M^2 reads in the basis $\{H_1^0, H_2^0, A^0\}$ [18]:

$$M^2 = \begin{pmatrix} \lambda_1 v^2 & \lambda_6 v^2 & -\text{Im}(\lambda_6) v^2 \\ \lambda_6 v^2 & M_{22}^2 + \frac{1}{2} v^2 (\lambda_3 + \lambda_4 + \lambda_5) & -\frac{1}{2} \text{Im}(\lambda_5) v^2 \\ -\text{Im}(\lambda_6) v^2 & -\frac{1}{2} \text{Im}(\lambda_5) v^2 & M_{22}^2 + \frac{1}{2} v^2 (\lambda_3 + \lambda_4 - \lambda_5) \end{pmatrix}. \quad (4.7)$$

In the CP-conserving limit, all parameters are real. The CP-odd scalar therefore decouples from the CP-even scalars. The physical scalars h (SM Higgs) and H (BSM scalar) are connected to H_1^0 and H_2^0 via the relation

$$\begin{pmatrix} h \\ H \end{pmatrix} = \begin{pmatrix} \cos(\alpha - \beta) & \sin(\alpha - \beta) \\ -\sin(\alpha - \beta) & \cos(\alpha - \beta) \end{pmatrix} \begin{pmatrix} H_1^0 \\ H_2^0 \end{pmatrix}, \quad (4.8)$$

where the mixing angle is given as

$$\sin(2(\alpha - \beta)) = \frac{2v^2 \lambda_6}{m_H^2 - m_h^2}. \quad (4.9)$$

4 The Two-Higgs-Doublet Model

In the alignment limit, $\alpha \approx \beta$ holds. In this case, H_1^0 becomes the SM Higgs h and H_2^0 is the new BSM CP-even scalar. The alignment limit also requires λ_6 to be zero and diagonalizes the mass matrix. The mass expressions for the scalars can therefore directly be read off from Eqs. 4.7 and A.42 to be:

$$\begin{aligned}
 m_h^2 &= \lambda_1 v^2 \\
 m_H^2 &= m_{22}^2 + \frac{v^2}{2}(\lambda_3 + \lambda_4 + \lambda_5) \\
 m_A^2 &= m_{22}^2 + \frac{v^2}{2}(\lambda_3 + \lambda_4 - \lambda_5) \\
 m_{H^\pm}^2 &= m_{22}^2 + \frac{v^2}{2}\lambda_3
 \end{aligned} \tag{4.10}$$

Now, the restrictions on the masses of the individual scalars can be discussed with respect to experimental data. Regarding a lower mass bound for the charged scalar, there are experimental constraints from collision experiments at the Large Electron-Positron Collider (LEP) [20] that require $m_{H^\pm} \geq 110$ GeV. Experiments that searched for a charged scalar with a mass below this threshold could not prove the existence. A detailed explanation of the derivation of this lower bound can be found in [19].

Further restrictions come from the extensively investigated decay of the Z -Boson $Z \rightarrow AH$ [21],[22]. The fact that this decay could not be detected suggests that both scalars can not be simultaneously lighter than the Z -boson with $m_Z \approx 91$ GeV. Further restrictions that have to be taken into account regarding the T-parameter, that plays a role in electroweak precision measurements. In order to favour these constraints, the choice of $m_{A^0} = m_{H^\pm}$ turns out to be convenient. Details on the T-parameter constraint are presented in [19].

Based on these restrictions, we assume the CP-even scalar to be in the light state. To give an outlook, this assumption will be further justified in the subsequent sections.

Besides the discussed lower bounds that are mostly motivated by experimental data, there are also perturbative restrictions arising from the coupling parameters from Eq. 4.10. From now on, we choose the CP-even scalar to be in the light state which allows the choice of $m_H = m_{22}$. This caused $\lambda_3 + \lambda_4 = -\lambda_5$ and consequently results in the following expressions:

$$\begin{aligned}
 m_H^2 &= m_{22}^2 \\
 m_A^2 &= m_H^2 - v^2\lambda_5 \\
 m_{H^\pm}^2 &= m_H^2 - \frac{v^2}{2}(\lambda_4 + \lambda_5)
 \end{aligned} \tag{4.11}$$

The assumption that $m_{A^0} = m_{H^\pm}$ forces $\lambda_4 = \lambda_5 \equiv \lambda$ to hold. If the mass of the light CP-even state is neglected, we obtain

$$m_{H^\pm}^2 = m_A^2 = -v^2\lambda \tag{4.12}$$

which puts an upper bound on the masses of the charged and the CP-odd scalar. This is due to perturbative conditions that require λ to be sufficiently small for convergence. Given $m_{H^\pm} = 110$ GeV, this leads to $\lambda = -0.2$. To avoid the risk of divergence, $|\lambda| \leq 2$ provides a suitable upper bound for perturbative convergence. Higher mass splittings would lead to larger values of λ . In order to avoid possible perturbative divergences for higher masses of the CP-odd scalar, it turns out to be convenient to use the lowest possible bound for the heavy states. In total, the mass hierarchy reads

$$m_{H^\pm} = m_A = m_H + 110 \text{ GeV}. \tag{4.13}$$

4.2 The Anomalous Magnetic Moment for Different Textures of Yukawa Couplings

Interactions between fermions and scalars are mediated via Yukawa couplings. The interaction Lagrangian in the 2HDM [23] is given as

$$-\mathcal{L} = \tilde{Y}\bar{\ell}_L H_1 \ell_R + Y\bar{\ell}_L H_2 \ell_R + \text{h.c.}, \tag{4.14}$$

4 The Two-Higgs-Doublet Model

where ℓ_L is a left handed doublet and ℓ_R is a right handed singlet. \tilde{Y} and Y are independent 3×3 matrices, containing the possible Yukawa couplings. All new scalars are contained in the second doublet H_2 . In conclusion, the first doublet and \tilde{Y} are responsible for giving mass to the SM leptons. The effective Lagrangian for the study of Δa_μ is then given by the terms arising from the second doublet as

$$-\mathcal{L}_y \supset \frac{1}{\sqrt{2}} \left([Y_{ij}^{H^0} H^0 + iY_{ij}^{A^0} A^0] \bar{\ell}_{Li} \ell_{Rj} + \bar{\ell}_{Rj} \ell_{Li} [Y_{ji}^{H^0} H^0 - iY_{ji}^{A^0} A^0] \right) + Y_{ij}^{H^+} \bar{\nu}_{Li} \ell_{Rj} H^+ + H^- \bar{\ell}_{Rj} \nu_{Li} Y_{ji}^{H^-}, \quad (4.15)$$

There are a total of four different Yukawa textures that are examined in the upcoming sections. In order to analyze different scenarios of interactions of the predicted BSM scalars with the leptons from the SM, different textures of the Yukawa coupling matrix are examined. Each scenario corresponds to different fermionic lines in the diagrams from Figs. 7 and 8. The form of the Yukawa matrix in the lepton sector takes the form of

$$Y_{ij} = \begin{pmatrix} Y_{ee} & Y_{e\mu} & Y_{e\tau} \\ Y_{\mu e} & Y_{\mu\mu} & Y_{\mu\tau} \\ Y_{\tau e} & Y_{\tau\mu} & Y_{\tau\tau} \end{pmatrix}, \quad (4.16)$$

where the first index refers to the virtual fermion in the loop and the second index to the incoming and outgoing fermion. The entries are taken to be real.

4.2.1 Texture 1: Muon-Muon Yukawa Coupling Matrix

The first case to be analysed contains a Yukawa matrix texture as follows:

$$Y_{ij} = \begin{pmatrix} 0 & 0 & 0 \\ 0 & Y_{\mu\mu} & 0 \\ 0 & 0 & 0 \end{pmatrix}. \quad (4.17)$$

This Yukawa interaction corresponds to the scenario in which the internal fermion line in Figs. 7 and 8 is represented by a muon. The goal is now to find expressions for the scalar and pseudoscalar couplings c_s and c_p by comparing the coefficients from the generalized Lagrangian in Eq. 3.1. This allows us to incorporate these expressions to the results for arbitrary models from Eqs. 3.27 and 3.30. We can incorporate the Yukawa texture in Eq. 4.15 and group everything together:

$$-L_y \supset \frac{1}{\sqrt{2}} \left([Y_{\mu\mu} H^0 + iY_{\mu\mu} A^0] \bar{\mu}_L \mu_R + \bar{\mu}_R \mu_L [H^0 Y_{\mu\mu} - iA^0 Y_{\mu\mu}] \right) + Y_{\mu\mu} \bar{\nu}_L \mu_R H^+ + H^- \bar{\mu}_R \nu_L Y_{\mu\mu}. \quad (4.18)$$

The charge of H^+ need to obey the charge conservation in the Feynman diagram in Fig. 7. Since the muon carries a charge of $q_\mu = -1$ and the charged scalar is singly charged, the fermion has to be neutral $q_F = 0$. This can either be realized by $q_{H^+} = -1$ and the momentum direction in clockwise direction or $q_{H^+} = +1$ and the momentum direction in the counterclockwise direction in the loop. The choice of $q_{H^+} = -1$ is made from now on. For that reason, the term associated with the H^- scalar will be omitted from this point because H^- would not add new contributions. With this considerations, the Lagrangian reduces to:

$$-L \supset \frac{1}{\sqrt{2}} \left(Y_{\mu\mu} (\bar{\mu}_L \mu_R + \bar{\mu}_R \mu_L) H^0 + iY_{\mu\mu} (\bar{\mu}_L \mu_R - \bar{\mu}_R \mu_L) A^0 \right) + Y_{\mu\mu} \bar{\nu}_L \mu_R H^+. \quad (4.19)$$

Inserting the projection operators (Appendix A.8) results in

$$-L \supset \frac{1}{2\sqrt{2}} Y_{\mu\mu} \bar{\mu} ((1 + \gamma^5) + (1 - \gamma^5)) \mu H^0 + \frac{1}{2\sqrt{2}} iY_{\mu\mu} \bar{\mu} ((1 + \gamma^5) - (1 - \gamma^5)) \mu A^0 + \frac{1}{2} Y_{\mu\mu} \bar{\nu}_{Li} (1 + \gamma^5) \mu H^+, \quad (4.20)$$

4 The Two-Higgs-Doublet Model

which can be simplified into

$$L \supset -\frac{1}{\sqrt{2}}Y_{\mu\mu}\bar{\mu}\mu H^0 - \frac{1}{\sqrt{2}}iY_{\mu\mu}\bar{\mu} \cdot \gamma^5 \mu \cdot A^0 - Y_{\mu\mu}\bar{\nu}_{Li}(1 + \gamma^5)\mu H^+. \quad (4.21)$$

From this reduced Lagrangian, explicit expressions for c_s and c_p can be obtained by comparing the coefficients with Eq. 3.1 after removing the fields:

$$\begin{aligned} \text{For } H^0 : c_s &= -\frac{1}{\sqrt{2}}Y_{\mu\mu}, c_p = 0 \\ \text{For } A^0 : c_s &= 0, c_p = -\frac{i}{\sqrt{2}}Y_{\mu\mu} \\ \text{For } H^+ : c_s &= -\frac{1}{2}Y_{\mu\mu}, c_p = -\frac{1}{2}Y_{\mu\mu}. \end{aligned} \quad (4.22)$$

This results can now be incorporated into the general equations Eqs. 3.27 and 3.30 to concretize for the individual contributions.

The contributions of the H^+ scalar will be embedded in the expression arising from Eq. 3.27. From now on, the variable z' is renamed as x .

$$\begin{aligned} \Delta a_\mu^{H^+} &= -\frac{q_H m_\mu^2}{8\pi^2} \int_0^1 dx \frac{|c_s|^2(x^3 - x^2 + \frac{m_F}{m_\mu}(x^2 - x)) + |c_p|^2(x^3 - x^2 - \frac{m_F}{m_\mu}(x^2 - x))}{m_\mu^2 x^2 + m_F^2(1-x) + (m_H^2 - m_\mu^2)x} \\ &\stackrel{4.22}{=} \frac{Y_{\mu\mu}^2}{16\pi^2} \int_0^1 dx \frac{x^3 - x^2}{x^2 + (\frac{m_F}{m_\mu})^2(1-x) + ((\frac{m_H}{m_\mu})^2 - 1)x} \\ &= \frac{Y_{\mu\mu}^2}{16\pi^2} \int_0^1 dx \frac{x^3 - x^2}{x^2 + (z_{H^+}^2 - 1)x} \quad \text{with } z_{H^+} = \frac{m_{H^+}}{m_\mu}. \end{aligned} \quad (4.23)$$

In the last step, the term proportional to $(m_F/m_\mu)^2$ was left out in the denominator. Under the constraint of charge conservation, the Feynman diagram from Fig. 7 allows in general multiply charged scalars and fermions. In the specific case of the 2HDM, the charged scalar is singly charged which requires the internal fermion to be neutral. Since the 2HDM only extends the scalar sector of the SM, the internal fermion line must be represented by a SM fermion with charge zero. The only particles with this property that come into question are neutrinos, which masses are negligible compared to the other leptons. Therefore, the contribution to the AMM from the charged scalar is independent of the fermion mass and conclusively remains the same for all discussed scenarios. The AMM contributions for the CP-even and CP-odd scalar are determined in a similar way by incorporating the expressions from Eq. 4.22 into Eq. 3.30. For H^0 we obtain

$$\begin{aligned} \Delta a_\mu^{H^0} &= -\frac{q_F m_\mu^2}{16\pi^2} \int_0^1 dx \frac{|c_s|^2(-x^3 + x^2 + \frac{m_F}{m_\mu}x^2) + |c_p|^2(x^3 + x^2 - \frac{m_F}{m_\mu}x^2)}{m_\mu^2 x^2 + m_{H^0}^2(1-x) + (m_F^2 - m_\mu^2)x} \\ &= \frac{Y_{\mu\mu}^2}{16\pi^2} \int_0^1 dx \frac{2x^2 - x^3}{x^2 + z_{H^0}^2(1-x)} \quad \text{with } z_{H^0} = \frac{m_H}{m_\mu}. \end{aligned} \quad (4.24)$$

We set $m_F = m_\mu$ in accordance with the selected Yukawa texture as stated in Eq. 4.57. With the same considerations, one can obtain the form of $\Delta a_\mu^{A^0}$:

$$\Delta a_\mu^{A^0} = \frac{Y_{\mu\mu}^2}{16\pi^2} \int_0^1 dx \frac{-x^3}{x^2 + z_{A^0}^2(1-x)} \quad \text{with } z_A = \frac{m_A}{m_\mu}. \quad (4.25)$$

The total contribution to the muon ($g-2$) anomaly then arises as a sum of all individual terms as:

$$\Delta a_\mu = \Delta a_\mu^{H^+} + \Delta a_\mu^{A^0} + \Delta a_\mu^{H^0}. \quad (4.26)$$

At this point we steer the focus back on the chosen mass hierarchy from Eq. 4.13 to examine the effect it has on the individual contributions to the AMM. We will now first examine the case in which all masses of the scalars labeled as m_S are equal:

$$m_S \equiv m_{H^0} = m_{A^0} = m_{H^+}. \quad (4.27)$$

4 The Two-Higgs-Doublet Model

By incorporating this assumption, the individual contributions from Eqs. 4.23-4.25 are visualized in Fig. 9 a). One can observe that the CP-even scalar is the only one that shows a global positive behaviour whereas the share from the CP-odd scalar is strictly negative. The charged scalar contributions shows an oscillatory behaviour in the range below m_μ . This is caused by the sign flip that occurs in the denominator in the lower proximity of m_μ . The important fact to recall is, that Δa_μ is in the positive direction. This observation raises the necessity to suppress the influence of the CP-odd and charged scalar. A suppression can be achieved by assuming the masses of the charged and CP-odd scalar to be larger than the CP-even scalar so that the denominator increases in the respective equations.

Embedding the mass hierarchy into the individual contributions obtains the result presented in Fig. 9 a). One can observe that the contributions of the CP-odd and charged scalar are significantly suppressed compared to the CP-even scalar. When a higher mass splitting of $\Delta m = 200$ GeV is applied, influence of the heavy states is even further degraded. The effect of different mass splittings on the total contribution only shows a diminished effect in the high mass domain. Since this does not notably change the total contribution, the choice of $\Delta m = 110$ GeV is suitable. The $Z \rightarrow AH$ condition gave us the freedom to choose, whether the CP-even or the CP-odd scalar occupies a heavy state. By choosing the CP-odd scalar to be heavy, the negative contribution is automatically suppressed. Hence, the chosen mass split from Eq. 4.13 turns out to be a good choice for this scenario.

At this point, it is possible make a statement on the role of the charged scalar. We showed that the contribution from the charged scalar is independent of the internal fermion in the loop of Fig 7. Due to the LEP constraint, the charged scalar is forced to occupy a heavy state which suppresses the contribution to the AMM. For that reason, the contribution from the charged scalar can be neglected for all the other cases that are about to be discussed.

The next step of the analysis includes a parameter space scan, in which different combinations of $Y_{\mu\mu}$ and m_H are tested for an agreement with Δa_μ in the 1σ and 2σ allowed region. The allowed Pairs are plotted in Fig. 10. The intervals for the parameters were chosen to be in the ranges of $Y_{\mu\mu} \in [10^{-4}, 1]$ and $m_H \in [10^{-2}, 10^3]$ GeV. A total of 20000 pairs of randomly selected values within the given ranges are tested. The integrals are numerically evaluated with the *scipy.integrate*-library in *Python*.

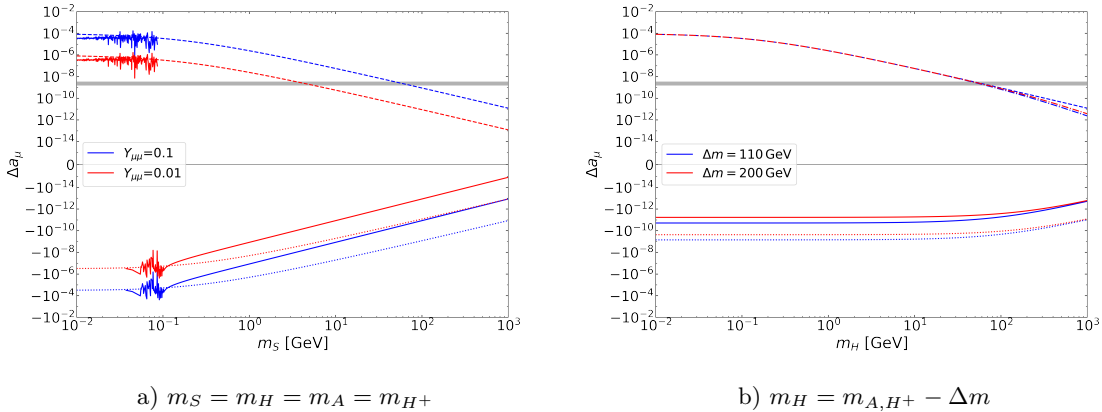


Figure 9: Individual contributions to Δa_μ from the charged scalar (continuous), the CP-even scalar (dashed) and the CP-odd scalar (dotted) from Eqs. 4.23-4.25. The sum of all contribution is marked with a dotted-dashed line in b). The oscillations belong exclusively to the charged scalar. In a), all masses of the scalars are equal. In b), two different mass splittings Δm are applied to the mass hierarchy. The Yukawa coupling was fixed to $Y_{\mu\mu} = 0.1$ in b). The gray shaded band indicates the 2σ region of Δa_μ .

4 The Two-Higgs-Doublet Model

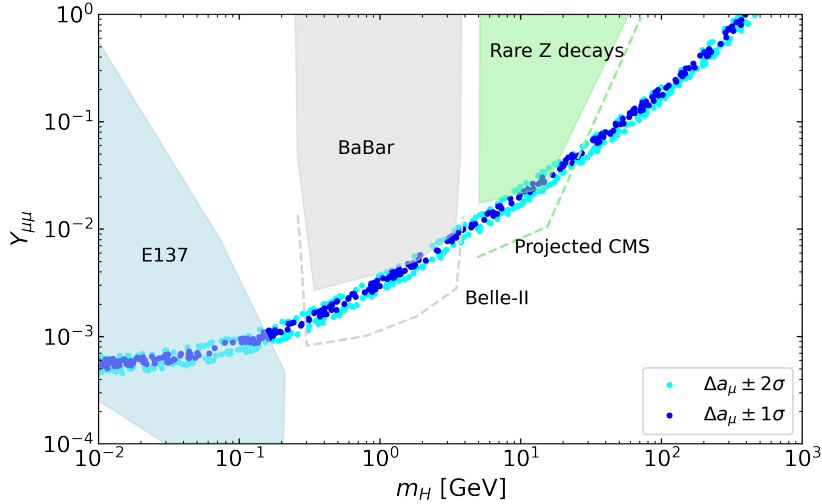


Figure 10: Parameter Space indicating the allowed combinations of the Yukawa coupling $Y_{\mu\mu}$ and m_H that are consistent with the 1σ and 2σ region of Δa_μ using Eq. 4.26 with the mass hierarchy from Eq. 4.13. Furthermore, the experimentally excluded regions from SLAC beam dump E137 (blue shaded) [24], BaBar (gray shaded) [25] and CMS (green shaded) [26] are visualized. Also shown is the projected sensitivity from Belle-II [27] (gray dotted line) and from CMS (green dotted line) that indicate a potentially excluded region by future experiments. The experimental data extracted from [28].

The shape of the graph can be substantiated by examining different cases in which the mass of the CP-even scalar is significantly smaller or larger than the muon mass. Considering the case in which $m_H \ll m_\mu$ holds, the term proportional to z_b^2 in the denominator of Eq. 4.24 can be neglected. This allows a simplification to:

$$\Delta a_\mu^{H^0 \ m_H \ll m_\mu} \approx \frac{Y_{\mu\mu}^2}{16\pi^2} \int_0^1 dx (2-x) = \frac{3Y_{\mu\mu}^2}{32\pi^2} \quad (4.28)$$

which is a constant with respect to m_H and explains the flattening tendency in the lower mass region of Fig. 10. The case in which $m_H \gg m_\mu$ holds suggests a neglect of the x^2 term in the denominator. However, this neglect would lead to a divergence of the integral and necessitate the inclusion of a tiny parameter in the denominator. For that reason, we make the assumption, that for high masses, the effect of m_H on the integral becomes so negligible, that we can extract the factor of z_H and the integral becomes a constant I such that:

$$\Delta a_\mu^{H^0 \ m_H \gg m_\mu} \approx \frac{Y_{\mu\mu}^2}{16\pi^2} \left(\frac{m_\mu}{m_H} \right)^2 \cdot I. \quad (4.29)$$

This approach explains the observed linear behaviour in the higher mass regions.

4.2.2 Texture 2: Tau-Muon Yukawa Coupling Matrix

The second scenario to be examined contains a flavor change in the internal line of the Feynman diagrams in Fig. 8. In this case, the incoming muon splits into a virtual τ and a neutral scalar from which the τ interacts with the photon from the electromagnetic field. As already discussed in the previous chapter, the contribution from the charged scalar is neglected. The Yukawa matrix texture takes the form of:

$$Y_{ij} = \begin{pmatrix} 0 & 0 & 0 \\ 0 & 0 & 0 \\ 0 & Y_{\tau\mu} & 0 \end{pmatrix}. \quad (4.30)$$

4 The Two-Higgs-Doublet Model

Incorporating this texture into the general Lagrangian from Eq. 4.15 and neglecting the terms arising from the charged scalar results in the following interaction Lagrangian:

$$-L_y \supset \frac{1}{\sqrt{2}} (\bar{\tau}_R \mu_L [Y_{\tau\mu} H^0 - i Y_{\tau\mu} A^0]). \quad (4.31)$$

Inserting the projection operators turns this into

$$-L_y \supset \frac{1}{2\sqrt{2}} (\tau [Y_{\mu\tau} H^0 - i Y_{\mu\tau} A^0] (1 - \gamma^5) \bar{\mu}). \quad (4.32)$$

Reading off the coefficients yields the following expressions for c_s and c_p :

$$\begin{aligned} \text{For } H^0: \quad c_s &= -\frac{1}{2\sqrt{2}} Y_{\mu\tau}, \quad c_p = \frac{1}{2\sqrt{2}} Y_{\mu\tau} \\ \text{For } A^0: \quad c_s &= \frac{i}{2\sqrt{2}} Y_{\mu\tau}, \quad c_p = -\frac{i}{2\sqrt{2}} Y_{\mu\tau} \end{aligned} \quad (4.33)$$

These can now be incorporated into the general expression from Eq. 3.30:

$$\begin{aligned} \Delta a_\mu(H^0, A^0) &= \frac{1}{8\pi^2} \int_0^1 dx \frac{|c_s|^2 (x^2 - x^3 + \frac{m_\tau}{m_\mu} x^2) + |c_p|^2 (x^2 - x^3 - \frac{m_\tau}{m_\mu} x^2)}{x^2 + z_b^2 (1-x) + (z_a^2 - 1)x} \\ &\stackrel{4.33}{=} \frac{Y_{\tau\mu}^2}{32\pi^2} \int_0^1 dx \frac{x^2 - x^3}{x^2 + z_b^2 (1-x) + (z_a^2 - 1)x}, \end{aligned} \quad (4.34)$$

where

$$z_a = \frac{m_\tau}{m_\mu} \text{ and } z_b = \frac{m_\phi}{m_\mu} \text{ with } \phi = H^0, A^0. \quad (4.35)$$

Combining the contributions from all scalars aggregates in

$$\Delta a_\mu = \frac{Y_{\tau\mu}^2}{32\pi^2} \left[G\left(\frac{m_\tau}{m_\mu}, \frac{m_H}{m_\mu}\right) + G\left(\frac{m_\tau}{m_\mu}, \frac{m_A}{m_\mu}\right) \right] \quad (4.36)$$

with

$$G(z_a, z_b) = \int_0^1 dx \frac{x^2 - x^3}{x^2 + (z_a^2 - 1)x + z_b^2(1-x)}. \quad (4.37)$$

First, it is important to clarify the choice of mass hierarchy. In this scenario, both contributions from the scalars are positive. For that reason, the constraint from the Z -decay leaves a free choice which of both scalars is taken to be light. However, in order to stay consistent with the $Y_{\mu\mu}$ -case, the same mass split as in Eq. 4.13 is incorporated and therefore degrades the share of the CP-odd scalar (Fig. 11 (right)). The effect of this mass splitting is visualized in Fig. 11.

4 The Two-Higgs-Doublet Model

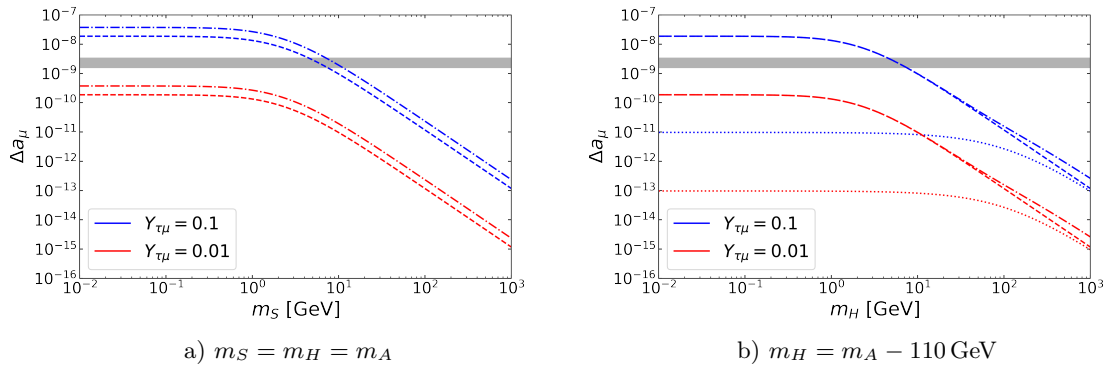


Figure 11: Individual contributions from Eq. 4.36 with equal masses for each scalar in a) and with the mass splitting from Eq. 4.13 in b). The dotted-dashed line refers to the sum of all terms in Eq. 4.36, the dotted line indicates the term from the CP-odd scalar and the dashed line visualizes the share from the CP-even scalar. The contributions are displayed for two different Yukawa couplings $Y_{\tau\mu}$. In the left figure, the contributions from the CP-even and CP-odd scalar overlap.

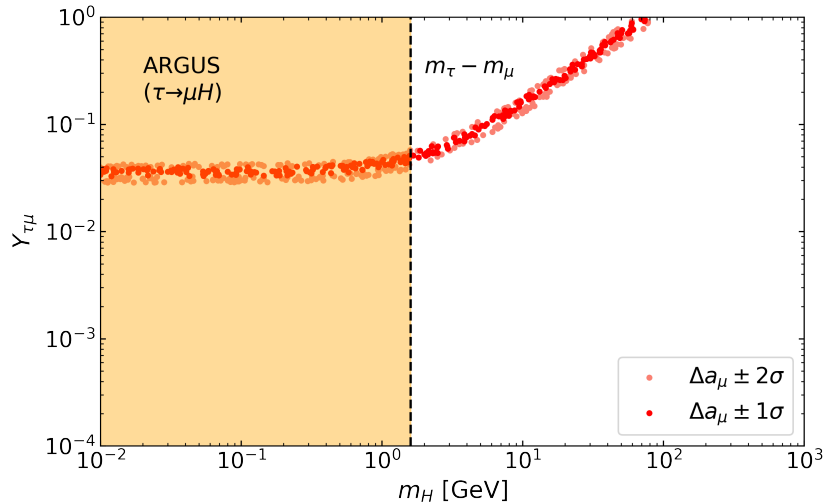


Figure 12: Parameter Space indicating the allowed combinations of the Yukawa coupling $Y_{\tau\mu}$ and m_H that are consistent with the 1σ and 2σ region of Δa_μ , using Eq. 4.36 with the mass hierarchy from Eq. 4.13. Furthermore, the experimentally excluded region from ARGUS [29] is shaded in orange. The ARGUS data are extracted from [30]. The dashed line marks the mass difference of the muon mass m_μ and the tau mass m_τ .

Based on Eq. 4.36 and the discussed mass hierarchy, a parameter scan is conducted in order to find combinations of m_H and $Y_{\tau\mu}$ that are in agreement with the value of Δa_μ (Fig. 12). Experiments from the ARGUS cooperation [29] could not verify the existence of the decay $\tau \rightarrow \mu H$. As a consequence, the mass of the CP-even scalar must have a larger mass than the difference of m_τ and m_μ since it seemingly does not participate in the decay of the tau. This result reduces the search area for the CP-odd scalar to the mass range above $m_\tau - m_\mu$.

In order to justify the shape of Fig. 12, we will examine different cases of the share from the CP-even scalar in Eq. 4.36. At first, we consider the case of $m_H \ll m_\tau$. Under this assumption we can disregard the term proportional to z_b^2 in the denominator because it is much smaller compared to z_a^2 . The comparably large value of z_a^2 also allows the neglect of the x^2 term as well as the

4 The Two-Higgs-Doublet Model

subtraction of -1. This allows

$$\begin{aligned}\Delta a_\mu &= \frac{Y_{\mu\tau}^2}{32\pi^2} \frac{1}{z_a^2} \int_0^1 dx x - x^2 \\ &= \frac{Y_{\mu\tau}^2}{192\pi^2} \left(\frac{m_\mu}{m_\tau}\right)^2\end{aligned}\quad (4.38)$$

as a simplification of the integral. The constant behaviour of the Yukawa coupling for masses m_H that are sufficiently smaller than m_τ becomes evident from this simplification. In the proximity of m_τ , $Y_{\mu\tau}$ shows a growing behaviour that persists in the higher mass regions. This can be reasoned by the inspection of the case $m_H \gg m_\tau$. In doing so, the $z_b^2(1-x)$ terms becomes increasingly larger than the $(z_a^2 - 1)x$ and the x^2 term in the denominator. We can therefore reduce Eq. 4.36 to

$$\begin{aligned}\Delta a_\mu &= \frac{Y_{\mu\tau}^2}{32\pi^2} \frac{1}{z_b^2} \int_0^1 dx \frac{x^2 - x^3}{1-x} \\ &= \frac{Y_{\mu\tau}^2}{32\pi^2} \left(\frac{m_\mu}{m_H}\right)^2 \int_0^1 dx \frac{x^2(1-x)}{(1-x)} \\ &= \frac{Y_{\mu\tau}^2}{96\pi^2} \left(\frac{m_\mu}{m_H}\right)^2.\end{aligned}\quad (4.39)$$

As seen in Fig. 12, this results in a linear relation between $Y_{\tau\mu}$ and m_H .

4.2.3 Texture 3: Muon-Tau and Tau-Muon Yukawa Coupling Matrix

In the third case, the Yukawa matrix takes the form of

$$Y_{ij} = \begin{pmatrix} 0 & 0 & 0 \\ 0 & 0 & Y_{\mu\tau} \\ 0 & Y_{\tau\mu} & 0 \end{pmatrix}.\quad (4.40)$$

This texture includes both the previously discussed case of an incident muon which transits into a virtual tau ($Y_{\tau\mu}$) in the loop as well as the scenario of an incident tau which transits to a muon in the loop in Fig. 8. The Lagrangian hence reads

$$-L_y \supset \frac{1}{\sqrt{2}} ([Y_{\mu\tau}H^0 + iY_{\mu\tau}A^0]\bar{\mu}_L\tau_R + \bar{\tau}_R\mu_L[Y_{\tau\mu}H^0 - iY_{\tau\mu}A^0])\quad (4.41)$$

This can be expanded to

$$-L_y \supset \frac{1}{2\sqrt{2}} ((Y_{\mu\tau}H^0\bar{\mu}(1+\gamma^5)\tau + Y_{\tau\mu}\bar{\tau}(1-\gamma^5)\mu H^0) + i(Y_{\mu\tau}A^0\bar{\mu}(1+\gamma^5)\tau - Y_{\tau\mu}\bar{\tau}(1-\gamma^5)\mu A^0)).\quad (4.42)$$

Comparing the coefficients results in the successive expressions:

$$\begin{aligned}\text{For } H^0 : \quad c_s &= -\frac{1}{2\sqrt{2}}(Y_{\mu\tau} + Y_{\tau\mu}), \quad c_p = -\frac{1}{2\sqrt{2}}(Y_{\mu\tau} - Y_{\tau\mu}) \\ \text{For } A^0 : \quad c_s &= -\frac{i}{2\sqrt{2}}(Y_{\mu\tau} - Y_{\tau\mu}), \quad c_p = -\frac{i}{2\sqrt{2}}(Y_{\mu\tau} + Y_{\tau\mu}).\end{aligned}\quad (4.43)$$

These can now be embedded in the expression of Eq. 3.30:

$$\begin{aligned}\Delta a_\mu &= -\frac{q_F m_\mu^2}{8\pi^2} \int_0^1 dx \frac{|c_s|^2(x^2 - x^3 + \frac{m_\tau}{m_\mu}x^2) + |c_p|^2(x^2 - x^3 - \frac{m_\tau}{m_\mu}x^2)}{m_\mu^2 x^2 + m_H^2(1-x) + (m_F^2 - m_\mu^2)x} \\ &\stackrel{m_\tau \gg m_\mu}{=} \frac{1}{8\pi^2} \left(\frac{m_\tau}{m_\mu}\right) \int_0^1 dx \frac{(|c_s|^2 - |c_p|^2)x^2}{x^2 + z_b^2(1-x) + (z_a^2 - 1)x}\end{aligned}\quad (4.44)$$

4 The Two-Higgs-Doublet Model

with

$$z_a = \frac{m_\tau}{m_\mu} \quad \text{and} \quad z_b = \frac{m_\phi}{m_\mu} \quad \text{with} \quad \phi = H^0, A^0. \quad (4.45)$$

In the second line of Eq. 4.44, we utilized the significantly larger mass ratio between the tau and muon allowing it to overshadow the terms $x^2 - x^3$ in nominator. We can now simplify the numerators for the individual particles with the expressions from eq. 4.43. For H^0 we have:

$$\begin{aligned} (|c_s|^2 - |c_p|^2)x^2 &= \frac{1}{8} \left((Y_{\mu\tau}^2 + 2Y_{\mu\tau}Y_{\tau\mu} + Y_{\tau\mu}^2) - (Y_{\mu\tau}^2 - 2Y_{\mu\tau}Y_{\tau\mu} + Y_{\tau\mu}^2) \right) x^2 \\ &= \frac{1}{2} Y_{\mu\tau}Y_{\tau\mu}x^2. \end{aligned} \quad (4.46)$$

For A^0 we receive analogously:

$$(|c_s^A|^2 + |c_p^A|^2)x^2 = -\frac{1}{2} Y_{\mu\tau}Y_{\tau\mu}x^2. \quad (4.47)$$

Merging everything together results in

$$\Delta a_\mu = \frac{Y_{\mu\tau}Y_{\tau\mu}}{16\pi^2} \left(\frac{m_\tau}{m_\mu} \right) \left[G \left(\frac{m_\tau}{m_\mu}, \frac{m_H}{m_\mu} \right) - G \left(\frac{m_\tau}{m_\mu}, \frac{m_A}{m_\mu} \right) \right], \quad (4.48)$$

where

$$G(z_a, z_b) = \int_0^1 dx \frac{x^2}{x^2 + (z_a^2 - 1)x + z_b^2(1 - x)}. \quad (4.49)$$

In Eq. 4.48, one observes that the term from the CP-odd scalar is negative. If both the mass of the CP-odd and CP-even scalar were equal, the terms would cancel out (Fig. 13 left). Referring to the condition from the Z -decay, this motivates the choice of the CP-odd scalar to occupy the heavy state and thus being consistent with the convention from Eq. 4.13. The effects of this mass splitting are depicted in Fig. 13. With our choice of hierarchy, the term from the CP-even scalar clearly dominates in the total contribution, whereas the CP-odd contribution is suppressed.

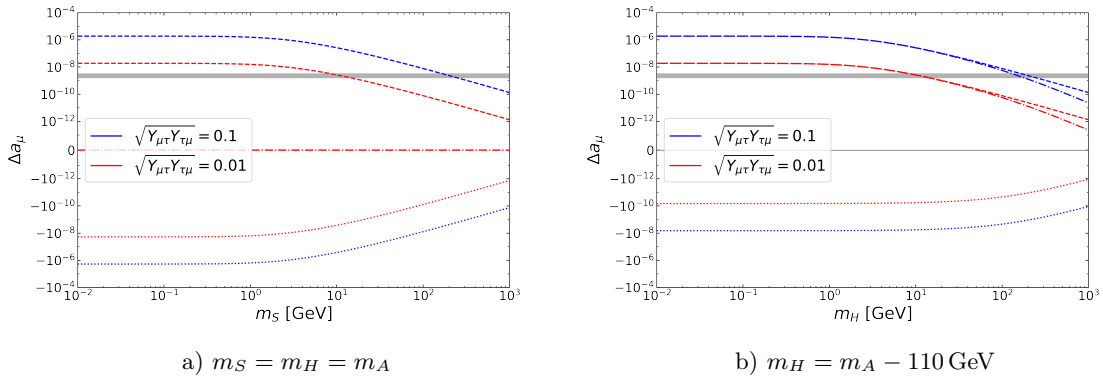


Figure 13: Individual contributions from Eq. 4.48 with equal masses for each scalar in a) and with the mass splitting from 4.13 in b). The dotted-dashed line refers to the sum of all terms in Eq. 4.36, the dotted line indicates the term from the CP-odd scalar and the dashed line visualizes the share from the CP-even scalar. The contributions are displayed for two different Yukawa couplings $\sqrt{Y_{\mu\tau}Y_{\tau\mu}}$. In b), the graphs from the CP-even scalar and the total contribution overlap but separate in the mass region above approximately 100 GeV. The gray shaded band indicates the 2σ region Δa_μ .

The scan of the associated parameter space is depicted in Fig. 14, which is based on Eq. 4.48. The two different Yukawa couplings are then combined to the geometric mean of $\sqrt{Y_{\mu\tau}Y_{\tau\mu}}$ for better comparability with the other scenarios. Moreover, the data from the ARGUS cooperation [29] exclude all masses below $m_\tau - m_\mu$ due to the undetected $\tau \rightarrow \mu H$ decay.

4 The Two-Higgs-Doublet Model

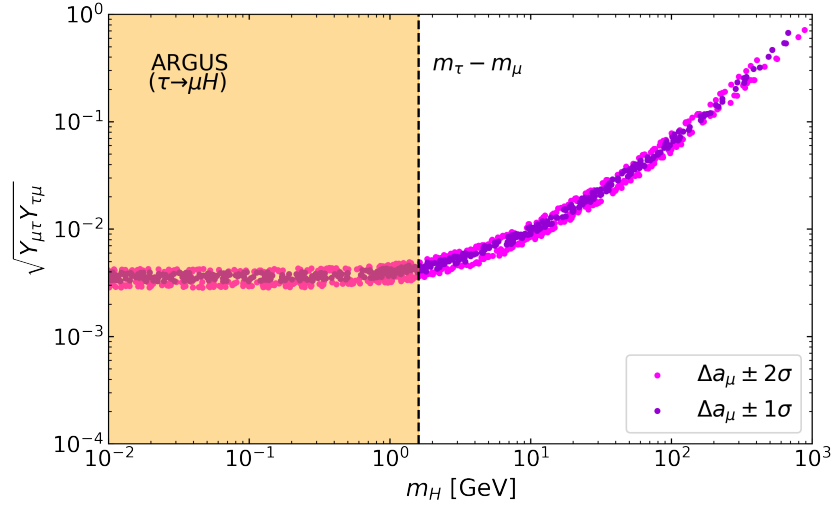


Figure 14: Parameter Space indicating the allowed combinations of the Yukawa coupling $\sqrt{Y_{\mu\tau}Y_{\tau\mu}}$ and m_H that are consistent with the 1σ and 2σ region of Δa_μ using Eq. 4.48 with the mass hierarchy from Eq. 4.13. The orange shaded region shows all masses that are excluded by the experimental data from the ARGUS cooperation [29]. The ARGUS data are extracted from [30]. The dashed line marks the mass difference of the muon mass m_μ and the tau mass m_τ .

For the discussion of the shape of the graph, only the CP-even scalar contribution is taken into account, as justified in Fig. 13 (right). Following the same argumentation as in Eq. 4.39 (neglecting x^2 , $z_b^2(1-x)$ and the subtraction of -1 in $(z_a^2 - 1)x$), the consideration of $m_H \ll m_\tau$ allows a reduction of the AMM contribution from the CP-even scalar to

$$\begin{aligned}\Delta a_\mu &= \frac{Y_{\mu\tau}Y_{\tau\mu}}{16\pi^2} \left(\frac{m_\mu}{m_\tau}\right) \int_0^1 dx x \\ &= \frac{Y_{\mu\tau}Y_{\tau\mu}}{32\pi^2} \left(\frac{m_\mu}{m_\tau}\right)\end{aligned}\quad (4.50)$$

which explains the observed constant behaviour in the low mass region. The attempt to find an analytical expression for the case of $m_H \gg m_\tau$ tempts the neglect of the term x^2 and $(z_a^2 - 1)x$ in the denominator. This assumptions would lead to a divergence at $x = 1$. Following a similar argumentation as for the $Y_{\mu\mu}$ texture, we assume that for sufficiently large masses, the integral I becomes independent of m_H and allows a simplification to:

$$\Delta a_\mu = \frac{Y_{\mu\tau}Y_{\tau\mu}}{16\pi^2} \left(\frac{m_\mu}{m_\tau}\right) \left(\frac{m_H}{m_\mu}\right)^2 \cdot I \quad (4.51)$$

This approximation can be justified by the shape of the graph in the higher mass regions.

4.2.4 Texture 4: Muon-Electron Yukawa Coupling Matrix

In last considered scenario, the internal loop line in Fig. 8 is represented by an electron. The corresponding Yukawa matrix texture reads

$$Y_{ij} = \begin{pmatrix} 0 & Y_{e\mu} & 0 \\ 0 & 0 & 0 \\ 0 & 0 & 0 \end{pmatrix}. \quad (4.52)$$

The derivation of the contribution to the AMM follows the exact same scheme as for the $Y_{\tau\mu}$ case in chapter 4.2.2. The only distinguishing property is now the mass of the electron m_e replacing m_τ in Eq. 4.36.

4 The Two-Higgs-Doublet Model

Conclusively, the total contribution to the AMM for this scenario is given as:

$$\Delta a_\mu = \frac{Y_{\mu e}^2}{32\pi^2} \left[G\left(\frac{m_e}{m_\mu}, \frac{m_H}{m_\mu}\right) + G\left(\frac{m_e}{m_\mu}, \frac{m_A}{m_\mu}\right) \right] \quad (4.53)$$

with

$$G(z_a, z_b) = \int_0^1 dx \frac{x^2 - x^3}{x^2 + (z_a^2 - 1)x + z_b^2(1 - x)}. \quad (4.54)$$

Both contributions to the AMM are positive. Hence, the Z -decay condition would leave a choice for the heavy state between the CP-even and CP-odd scalar (see Fig. 15 (left)). To preserve consistency through all scenarios, once again the same mass hierarchy is chosen as introduced in Eq. 4.13 (see Fig. 15 (right)). One can observe that the contribution to the AMM is negative for scalar masses below the muon mass. The graphs show an oscillating behavior in the lower proximity of m_μ and becomes positive for higher masses. This observation becomes also notable in the corresponding parameter space depicted in Fig. 16.

The parameter space scan reveals a cut-off for masses below m_μ . To explain this, we can examine the case of $m_H \ll m_\mu$ in Eq. 4.53. In this context, we can disregard the $z_b^2(1 - x)$ and the $z_a^2 x$ in the denominator which then gives

$$\begin{aligned} \Delta a_\mu &= \frac{Y_{e\mu}^2}{32\pi^2} \int_0^1 dx \frac{x^2 - x^3}{x^2 - x} \\ &= \frac{Y_{e\mu}^2}{32\pi^2} \int_0^1 dx \frac{-x(x - 1)}{x - 1} \\ &= -\frac{Y_{e\mu}^2}{64\pi^2}. \end{aligned} \quad (4.55)$$

In the lower mass region of m_H , the contribution therefore becomes negative and therefore explains the observed cut-off in the parameter space as well as the oscillations in Fig. 15 which occur owing to the sign flip in denominator. On the other hand, the consideration of $m_H \gg m_\mu$ allows the construction of the following expression:

$$\begin{aligned} \Delta a_\mu &= \frac{Y_{e\mu}^2}{32\pi^2} \int_0^1 dx \frac{x^2 - x^3}{z_b^2(1 - x)} \\ &= \frac{Y_{e\mu}^2}{32\pi^2} \left(\frac{m_\mu}{m_H}\right)^2 \int_0^1 dx \frac{x^2(1 - x)}{1 - x} \\ &= \frac{Y_{e\mu}^2}{96\pi^2} \left(\frac{m_\mu}{m_H}\right)^2. \end{aligned} \quad (4.56)$$

This result agrees exactly with the high mass approximation from the $Y_{\tau\mu}$ scenario in Eq. 4.38.

4 The Two-Higgs-Doublet Model

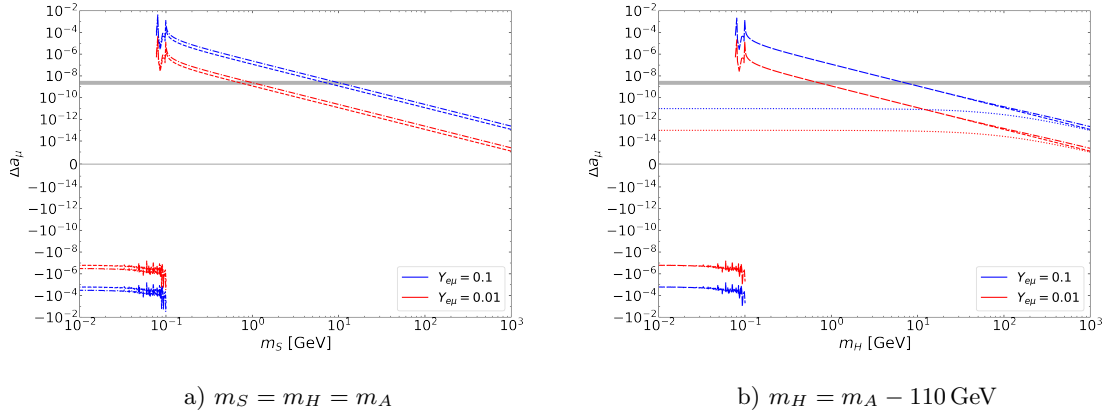


Figure 15: Individual contributions to Δa_μ from the CP-even scalar (dashed) and the CP-odd scalar (dotted) as well as the sum of both contributions (dotted-dashed) from Eq. 4.53 for two different Yukawa couplings $Y_{e\mu}$. The graphs from the CP-even scalar and the CP-odd scalar overlap in a). In b), the graphs from the total contribution and the CP-even scalar overlap and separate only slightly in the high mass region. The gray shaded band indicates the 2σ region of Δa_μ .

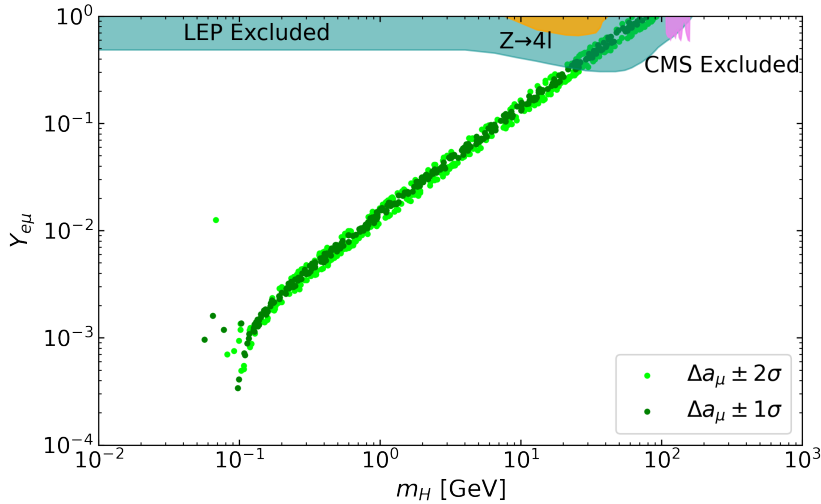


Figure 16: Parameter scan of texture 4 based on Eq. 4.53 with the mass hierarchy from Eq.4.13 indicating the allowed parameter combinations of $Y_{e\mu}$ and m_H for an agreement with 1σ and 2σ region of Δa_μ . The experimentally excluded regions from LEP (dark cyan) [31], $Z \rightarrow 4l$ (yellow) [32] and CMS (magenta) [33] are also displayed. The experimental data are extracted from [34].

4.2.5 Direct Comparison of the Parameter Spaces

To sum up the results of the individual scenarios, all parameter spaces are directly compared to each other in Fig. 17. The experimental constraints are not included, as they are only valid for the respective scenario in which they have been introduced.

In the mass region of $m_H < m_\mu$, texture 4 is the only one that shows no allowed parameter combinations due to the discussed negative share to the AMM (Eq. 4.55). The direct comparison of the second and third case shows, that two non-vanishing matrix entries allow lower Yukawa couplings by approximately one order of magnitude which becomes clear from the direct comparison of the low mass approximations (Eqs. 4.39, 4.50). The first texture allows the weakest Yukawa coupling compared to textures 2 and 3 since m_τ leads to increased denominators which reduce the

4 The Two-Higgs-Doublet Model

contribution.

In the range of $m_\mu < m_H < m_\tau$, the graphs for texture 2 and 3 remain constant up to m_τ (Eqs. 4.39, 4.50). The Yukawa coupling for texture 4 starts to grow proportional to m_H (Eq. 4.56). The graph of texture 1 also shows a growing trend that is modulated by the integral expression (Eq. 4.29).

In the higher mass range of $m_H > m_\tau$, the graphs from texture 2 and 4 overlap as the high mass approximations suggest (Eqs. 4.38, 4.56). The graphs from texture 1 and 3 strive to a linear trend as the graphs from textures 2 and 4. This reveals that the high mass approximations for texture 1 and texture 3 (Eqs. 4.29, 4.51) are valid in the high mass range.

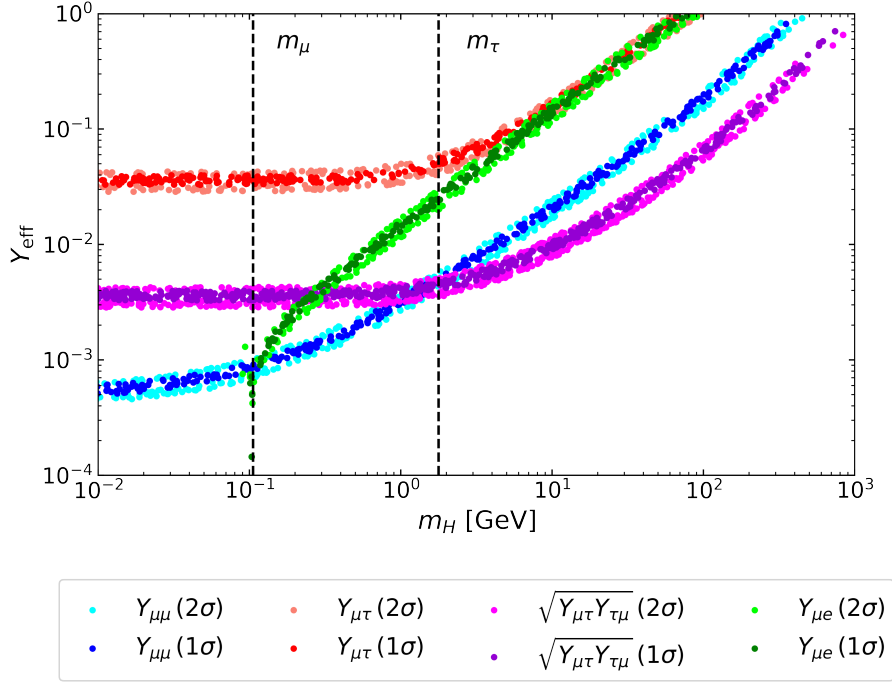


Figure 17: Combined parameter scans from Figs. 10, 12, 14 and 16. Y_{eff} is a placeholder for the specific Yukawa couplings listed in the legend. All scans refer to the allowed 1σ and 2σ region of Δa_μ . The dashed lines indicate the masses of the muon m_μ and the tau m_τ .

The texture of

$$Y_{ij} = \begin{pmatrix} 0 & Y_{e\mu} & 0 \\ Y_{\mu e} & 0 & 0 \\ 0 & 0 & 0 \end{pmatrix}. \quad (4.57)$$

has not been included in the analysis. We would expect the same expression as for the $\mu\tau - \tau\mu$ -interaction (Eq. 4.48) with m_e replacing m_τ . Since the mass of the electron is much lower than m_μ , the term $\frac{m_e}{m_\mu} x^2$ would become insignificant in the nominator, leading to the nominator of $x^2 - x^3$. This would give us the same result as for the $Y_{e\mu}$ texture besides the replacement of $Y_{e\mu} \rightarrow \sqrt{Y_{e\mu}^2 + Y_{\mu e}^2}$ since the crossing terms would vanish. Hence this case would add no new results.

5 Conclusion

In this thesis, the muon $g - 2$ anomaly was studied in the 2HDM, one of the simplest extensions to the Standard Model. After a brief introduction on the basics of the experimental determination of a_μ , the g -factor was calculated both in the context of the Dirac equation and the transition amplitude arising from a tree level Feynman diagram. The parameterization of the Feynman amplitude could be generalized by the introduction of form factors. Here we could show that the AMM is proportional to the magnetic form factor. With the goal of extracting this magnetic form factor, the one-loop QED contribution was calculated, yielding the largest contribution to the AMM. The subsequent step involved a generalized calculation for a one-loop electroweak contribution, which enables the application of arbitrary models. The results have been cross-checked with the literature and have been reproduced with *package-X* in *Mathematica*.

The model of choice was the 2HDM. In the CP-conserving scenario and the alignment limit, we obtained three new scalar particles: a CP-even scalar H^0 , a CP-odd scalar A^0 , and a charged scalar H^\pm . The interactions of these particles with the fermions from the SM have been studied in detail by analyzing a total of four different possible Yukawa textures. For each scenario, the general results from the electroweak one-loop calculation have been adjusted by determining the scalar and pseudoscalar coefficients from a direct comparison with the associated interaction Lagrangian. Throughout all scenarios, a mass hierarchy between the particles of $m_{H^\pm} = m_{A^0} = m_{H^0} + 110 \text{ GeV}$ was chosen which was motivated by experimental constraints and mathematical conditions. With the applied mass split, the contribution arising from the light CP-even state turned out to be most dominant one for each Yukawa matrix texture. For each scenario, a parameter scan was conducted in order to filter for combinations of parameters that add the missing contribution of Δa_μ . The parameter scans have been supplemented with experimental data that excluded parts of the theoretically predicted regions, hence allowing a more targeted experimental search.

Overall, the numerical analysis emphasized the importance of close cooperation between theoretical and experimental physics. It became clear how a theoretical prediction can steer the direction of experimental research and vice versa. Moreover, the work revealed how seemingly insignificant properties in nature can contribute to revealing the most fundamental secrets of physics. A deviation of 5σ between theory and experiment is regarded as a new discovery in particle physics. The muon $g - 2$ anomaly already exceeds this benchmark and therefore presents tantalizing evidence for potential new physics beyond the standard model. It remains to be seen how future experiments will be able to directly detect the new particles. On the other side, theoretical prediction can be further precised by focusing on lattice QCD contributions, which are at the center of recent research.

A Appendix

A Appendix

A.1 Gamma Matrices

The 4x4 gamma matrices in Dirac representation are given as [13]:

$$\gamma^0 = \begin{pmatrix} \mathbb{1}_{2 \times 2} & 0 \\ 0 & -\mathbb{1}_{2 \times 2} \end{pmatrix}, \quad \gamma^i = \begin{pmatrix} 0 & \sigma_i \\ -\sigma_i & 0 \end{pmatrix} \quad (\text{A.1})$$

where σ_i are the Pauli-matrices:

$$\sigma_1 = \begin{pmatrix} 0 & 1 \\ 1 & 0 \end{pmatrix}, \quad \sigma_2 = \begin{pmatrix} 0 & -i \\ i & 0 \end{pmatrix}, \quad \sigma_3 = \begin{pmatrix} 1 & 0 \\ 0 & -1 \end{pmatrix}. \quad (\text{A.2})$$

The Pauli matrices fulfill the relation that

$$\sigma_i \sigma_j = \delta_{ij} + i \varepsilon_{ijk} \sigma_k \quad (\text{A.3})$$

such as the identity

$$(\mathbf{a} \cdot \boldsymbol{\sigma})(\mathbf{b} \cdot \boldsymbol{\sigma}) = \mathbf{a} \cdot \mathbf{b} + i \boldsymbol{\sigma}(\mathbf{a} \times \mathbf{b}) \quad (\text{A.4})$$

which can be directly proven:

$$\begin{aligned} (\mathbf{a} \cdot \boldsymbol{\sigma})(\mathbf{b} \cdot \boldsymbol{\sigma}) &= (a_i \sigma_i)(b_j \sigma_j) = a_i b_j \sigma_i \sigma_j \stackrel{\text{A.3}}{=} a_i b_j (\delta_{ij} + i \varepsilon_{ijk} \sigma_k) \\ &= \mathbf{a} \cdot \mathbf{b} + i \sigma_k \varepsilon_{kij} a_i b_j = \mathbf{a} \cdot \mathbf{b} + i \boldsymbol{\sigma}(\mathbf{a} \times \mathbf{b}). \end{aligned} \quad (\text{A.5})$$

The γ -matrices obey the Clifford-Algebra

$$\{\gamma^\mu, \gamma^\nu\} = 2g^{\mu\nu} = 2 \text{diag}(1, -1, -1, -1). \quad (\text{A.6})$$

The commutator is defined as

$$\sigma^{\mu\nu} = \frac{i}{2} [\gamma^\mu, \gamma^\nu]. \quad (\text{A.7})$$

An useful identity can be derived for the components $\mu = 1, 2, 3$. Starting with explicit matrix multiplication, one can find that

$$\begin{aligned} \sigma_{ij} &= \frac{i}{2} \begin{pmatrix} -\sigma_i \sigma_j + \sigma_j \sigma_i & 0 \\ 0 & -\sigma_i \sigma_j + \sigma_j \sigma_i \end{pmatrix} \\ &= \frac{-i}{2} [\sigma_i, \sigma_j] \mathbb{1} \\ &= \frac{-i}{2} (\delta_{ij} + i \varepsilon_{ijk} \sigma_k - \delta_{ji} - i \varepsilon_{jik} \sigma_k) \mathbb{1} \\ &= \varepsilon_{ijk} \sigma_k \mathbb{1}. \end{aligned} \quad (\text{A.8})$$

Important properties of the γ -matrices include [13],P.820:

$$\begin{aligned} \gamma^\mu \gamma_\mu &= 4 \\ \gamma^\mu \gamma^\nu \gamma_\mu &= -2\gamma^\nu \\ \gamma^\mu \gamma^\nu \gamma^\rho \gamma_\mu &= 4g^{\nu\rho} \\ \gamma^\mu \gamma^\nu \gamma^\rho \gamma^\sigma \gamma_\mu &= -2\gamma^\sigma \gamma^\rho \gamma^\nu. \end{aligned} \quad (\text{A.9})$$

The γ^5 matrix is introduced as

$$\gamma^5 = i\gamma^0 \gamma^1 \gamma^2 \gamma^3 \quad (\text{A.10})$$

which anticommutes with all other γ matrices

$$\{\gamma^5, \gamma^\mu\} = 0 \quad \text{for } \mu = 0, 1, 2, 3. \quad (\text{A.11})$$

Furthermore, γ^5 satisfies

$$(\gamma^5)^2 = \mathbb{1}. \quad (\text{A.12})$$

A Appendix

A.2 Feynman Rules

In this chapter, the Feynman rules that are used in the calculations are listed. The rules are taken from [12], P.149.

For external lines:

$$\begin{aligned} \text{Incoming Fermion: } & \begin{array}{c} \xrightarrow{p} \\ \bullet \end{array} = u(p) \\ \text{Outgoing Fermion: } & \begin{array}{c} \xrightarrow{p} \\ \bullet \end{array} = \bar{u}(p) \end{aligned}$$

For internal lines:

$$\begin{aligned} \text{Spin 0 Boson: } & \begin{array}{c} \xrightarrow{p} \\ \bullet \text{---} \bullet \end{array} = \frac{i}{p^2 - m^2} \\ \text{Spin } \frac{1}{2} \text{ Fermion: } & \begin{array}{c} \xrightarrow{p} \\ \bullet \text{---} \bullet \end{array} = \frac{i(\not{p} + m)}{p^2 - m^2} \\ \text{Spin 1 Photon: } & \begin{array}{c} \xrightarrow{p} \\ \bullet \text{---} \bullet \end{array} = \frac{-ig^{\mu\nu}}{p^2} \end{aligned}$$

Vertex factors:

$$\begin{aligned} \text{Photon, Spin } \frac{1}{2} \text{ fermion: } & \begin{array}{c} \swarrow \quad \searrow \\ \quad \downarrow \\ \quad \downarrow \\ \quad \downarrow \end{array} = -ie\gamma^\mu \\ \text{Photon, Spin 0 boson: } & \begin{array}{c} \swarrow \quad \searrow \\ \quad \downarrow \\ \quad \downarrow \\ \quad \downarrow \end{array} = -iq_H e(p + p') \end{aligned}$$

A.3 Gordon Identity

The Gordon Identity is used in various calculations throughout this thesis. The identity to proof is given as

$$\bar{u}(q_2)\gamma^\mu u(q_1) = \frac{1}{2m}\bar{u}_f((p_f + p_i)^\mu + i\sigma^{\mu\nu}(p_f - p_i)_\nu)u_i. \quad (\text{A.13})$$

In doing so, we first have a look at the commutator and the anti-commutator relations of the Gamma-Matrices (see Appendix A.1):

$$\frac{i}{2}[\gamma^\mu, \gamma^\nu] = \sigma^{\mu\nu} \quad \text{and} \quad \{\gamma^\mu, \gamma^\nu\} = 2g^{\mu\nu} \quad (\text{A.14})$$

By utilizing the commutator and anti-commutator relation we can derive two expressions for $i\sigma^{\mu\nu}$:

$$\begin{aligned} i\sigma^{\mu\nu} &= -\frac{1}{2}[\gamma^\mu, \gamma^\nu] \\ &= -\frac{1}{2}(\gamma^\mu\gamma^\nu - \gamma^\nu\gamma^\mu) \\ &\stackrel{\text{A.6}}{=} -\frac{1}{2}(\gamma^\mu\gamma^\nu - (2g^{\mu\nu} - \gamma^\mu\gamma^\nu)) \\ &= -\frac{1}{2}(2(\gamma^\mu\gamma^\nu - g^{\mu\nu})) \\ &= g^{\mu\nu} - \gamma^\mu\gamma^\nu. \end{aligned} \quad (\text{A.15})$$

A Appendix

Similarly,

$$\begin{aligned}
i\sigma^{\mu\nu} &= g^{\mu\nu} - \gamma^\mu\gamma^\nu \\
&\stackrel{A.6}{=} g^{\mu\nu} - (2g^{\mu\nu} - \gamma^\mu\gamma^\nu) \\
&= \gamma^\nu\gamma^\mu - g^{\mu\nu}.
\end{aligned} \tag{A.16}$$

The reason why we need two representations of the same $i\sigma^{\mu\nu}$ term will become evident in a moment. We will now exclusively look at the $i\sigma^{\mu\nu}(p_f - p_i)_\nu$ term surrounded by the spinors \bar{u}_f and u_i .

$$\begin{aligned}
\bar{u}_f(i\sigma^{\mu\nu}(p_f - p_i)_\nu)u_i &\stackrel{A.15,A.16}{=} \bar{u}_f((\gamma^\nu\gamma^\mu - g^{\mu\nu})p_{f,\nu} - (g^{\mu\nu} - \gamma^\mu\gamma^\nu)p_{i,\nu})u_i \\
&= \bar{u}_f(\not{p}_f\gamma^\mu - p_f^\mu) - (p_i^\mu - \gamma^\mu\not{p}_i)u_i \\
&\stackrel{2.35}{=} \bar{u}_f(2m\gamma^\mu - (p_f + p_i)^\mu)u_i
\end{aligned} \tag{A.17}$$

The two representations of $i\sigma^{\mu\nu}$ were necessary in order to apply both the Dirac and the adjoint Dirac-Equation. Rearranging the terms yields the well known form of

$$\bar{u}(q_2)\gamma^\mu u(q_1) = \frac{1}{2m}\bar{u}_f((p_f + p_i)^\mu + i\sigma^{\mu\nu}(p_f - p_i)_\nu)u_i. \tag{A.18}$$

A.4 Feynman Parametrization

The Feynman parametrization is a useful tool to simplify denominators consisting of products by introducing an additional integral. The most general form of the is parametrization is [[35],P.497]

$$\frac{1}{\prod_{i=1}^n A_i} = (n-1)! \int_0^1 du_1 \dots \int_0^1 du_n \frac{\delta(1 - \sum_{k=1}^n u_k)}{(\sum_{k=1}^n u_k A_k)^n}. \tag{A.19}$$

The delta-function always constraints the Feynman parameters to obey:

$$\sum_{k=1}^n u_k = 1 \tag{A.20}$$

The $n = 3$ case is particularly significant for the computations in this thesis, as the one-loop diagrams contain a total of three propagators. Therefore, the proof of the $n = 3$ case is portrayed in the following way:

$$\begin{aligned}
\frac{1}{ABC} &\stackrel{!}{=} 2 \int_0^1 dx dy dz \delta(x + y + z - 1) \frac{1}{(xA + yB + zC)^3} \\
&= 2 \int_0^1 dx \int_0^{1-x} dy \frac{1}{(xA + yB + (1-x-y)C)^3} \\
&= 2 \int_0^1 dx \int_0^{1-x} dy \frac{1}{((A-C)x + (B-C)y + C)^3} \quad \Big|_{u = (A-C)x + (B-C)y + C} \\
&= \frac{2}{B-C} \int_0^1 dx \int_{(A-C)x+C}^{(A-B)x+B} du \frac{1}{u^3} \\
&= \frac{1}{B-C} \int_0^1 dx \left(\frac{1}{((A-C)x+C)^2} - \frac{1}{((A-B)x+B)^2} \right) \quad \Big|_{\text{sub}} \\
&= \frac{1}{(B-C)(A-C)} \int_C^A dt_1 \frac{1}{t_1^2} - \frac{1}{(B-C)(A-B)} \int_B^A dt_2 \frac{1}{t_2^2} \\
&= \frac{1}{(B-C)(A-C)} \left(\frac{A-C}{AC} \right) - \frac{1}{(B-C)(A-B)} \left(\frac{A-B}{AB} \right) \\
&= \frac{1}{A(B-C)} \left(\frac{1}{C} - \frac{1}{B} \right) = \frac{1}{ABC}.
\end{aligned} \tag{A.21}$$

A Appendix

A.5 Dimensional Regularization and Wick rotations

In particle physics, the computation of loop diagrams involves integrals of the form

$$I_n(\Delta) = \int d^D p \frac{1}{(p_\mu p^\mu - A + i\varepsilon)^n} = \int d^D p \frac{1}{(p_0^2 - \vec{p}^2 - A + i\varepsilon)^n}. \quad (\text{A.22})$$

Integrals of this kind face the risk of becoming divergent in four dimensions. The tool of dimensional regularization [36] addresses these possible divergences by the introduction of continuous dimensions D . In order to do so, an infinitesimal parameter $\varepsilon > 0$ is introduced. At the end of the calculation, we can perform the limit $D = (4 - \varepsilon)_{\varepsilon \rightarrow 0}$ in order to obtain the result for the four-dimensional space-time of our universe. The following proof only covers the superficial aspects of complex analysis. Considering eq. A.22, there are two poles at $p_0 = \pm \sqrt{\vec{p}^2 - A + i\varepsilon}$. The $+i\varepsilon$ shifts the poles in the complex plane as seen in fig. 18. The Cauchy integral theorem, states, the the closed contour integral over a holomorphic function $f(z)$ vanishes :

$$\oint_C f(z) dz = 0 \quad (\text{A.23})$$

A possible contour is depicted in Fig. 18. The integration path can be split up into four segments: two segments along the real and imaginary axis and two bow segments. The bow segments vanish since they are stretched to infinity when we integrate over the whole momentum space. The remaining segments are along the real and the imaginary axis.

$$\int_{-\infty}^{+\infty} f(k_0, \mathbf{k}) dk_0 + \int_{+i\infty}^{-i\infty} f(k_0, \mathbf{k}) dk_0 = 0 \quad (\text{A.24})$$

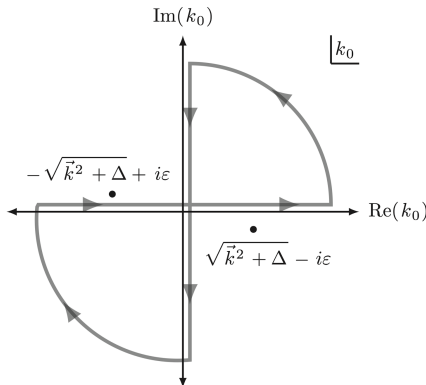


Figure 18: Schematic visualization of the integration path over k_0 in the complex plane. Taken from [13], P.824.

Hence, we showed the equivalence of both integration paths which allows us to perform a Wick rotation. A Wick rotation allows an transition from a Minkowski metric to a euclidean metric by introducing a complex 0th component in the four-vector. The calculation of the integral from Eq.

A Appendix

A.22 can now be performed:

$$\begin{aligned}
I_n(A) &= \int d^D p \frac{1}{(p_0^2 - \mathbf{p}^2 - A + i\varepsilon)^n} \quad \left| p_0 = ip_{E,0}, \quad p_E^2 = p_{E,0}^2 + \mathbf{p}_E^2 \right. \\
&= i(-1)^n \int d^D p \frac{1}{(p_E^2 + A - i\varepsilon)^n} \quad \left| \text{use spherical coordinates} \right. \\
&= i(-1)^n \int d\Omega_D \int_0^\infty dp_E \frac{p_E^{D-1}}{(p_E^2 + A - i\varepsilon)^n} \quad \left| x = p_E^2 \right. \\
&= \frac{i}{2}(-1)^n \int d\Omega_D \int_0^\infty dx \frac{1}{\sqrt{x}} \frac{x^{\frac{1}{2}(D-1)}}{(x + A - i\varepsilon)^n} \\
&= \frac{i}{2}(-1)^n \int d\Omega_D \int_0^\infty dx \frac{x^{\frac{D}{2}-1}}{(x + A - i\varepsilon)^n} \quad \left| y = \frac{A - i\varepsilon}{x + A - i\varepsilon} \right. \\
&= \frac{i}{2}(-1)^n \int d\Omega_D \int_1^0 dy - (A - i\varepsilon) \frac{1}{y^2} \frac{((A - i\varepsilon)(\frac{1}{y} - 1))^{\frac{D}{2}-1}}{(\frac{1}{y}(A - i\varepsilon))^n} \\
&= \frac{i}{2}(-1)^n (A - i\varepsilon)^{\frac{D}{2}-n} \int d\Omega_D \int_0^1 dy \quad y^{n-\frac{D}{2}-1} (1-y)^{\frac{D}{2}-1}. \tag{A.25}
\end{aligned}$$

At this point, we use that the angular component of this integral is

$$\int d\Omega_D = \frac{2\pi^{\frac{D}{2}}}{\Gamma(D)} \tag{A.26}$$

with the Γ -function. Furthermore, we can identify the Beta- Function that is given as:

$$B(z_1, z_2) = \int_0^1 y^{z_1-1} (1-y)^{z_2-1}. \tag{A.27}$$

The Beta function fulfills the relation:

$$B(z_1, z_2) = \frac{\Gamma(z_1)\Gamma(z_2)}{\Gamma(z_1 + z_2)}. \tag{A.28}$$

Thus, we can express Eq. A.25 as

$$I_n(A) = i(-1)^n (A - i\varepsilon)^{\frac{D}{2}-n} \frac{\pi^{\frac{D}{2}}}{\Gamma(\frac{D}{2})} \frac{\Gamma(n - \frac{D}{2})\Gamma(\frac{D}{2})}{\Gamma(n)} = i(-1)^n (A - i\varepsilon)^{\frac{D}{2}-n} \pi^{\frac{D}{2}} \frac{\Gamma(n - \frac{D}{2})}{\Gamma(n)}. \tag{A.29}$$

When considering the case of our four-dimensional space-time, we can set $D = 4 - \varepsilon$ and take the limit of $\varepsilon \rightarrow 0$, resulting in

$$\lim_{\varepsilon \rightarrow 0} I_n(A) = i(-1)^n A^{2-n} \pi^2 \frac{\Gamma(n-2)}{\Gamma(n)} \tag{A.30}$$

For the case of $n = 3$ which is of particular interest for the calculations, we have

$$I_3(A) = \frac{-i\pi^2}{2A}. \tag{A.31}$$

A.6 Reproduction of the Electroweak Contributions Using *package-X*

The calculation of the electroweak contributions from sections 3.2 and 3.3 can be reproduced with the open source *Mathematica* extension *Package-X* [7]. After the installation, the package is initialized with the command:

```
In[1]:= <<X
```

Now, we have to declare the Feynman parameters x, y and z to be Lorentz scalars so that they are not interpreted as four-vectors:

A Appendix

```
In[2]:= LScalarQ[x]=True;
        LScalarQ[y]=True;
        LScalarQ[z]=True;
```

Furthermore, we need to define the kinematic arguments by making use of the on-shell conditions:

$$\begin{aligned}
 p^2 &= (q_2 - q_1)^2 = q_2^2 + q_1^2 - 2q_2q_1 = 2m^2 - 2q_2q_1 \quad \Rightarrow \quad q_2q_1 = m^2 - \frac{p^2}{2} \\
 q_1^2 &= (q_2 - p)^2 = q_2^2 + p^2 - 2q_2p \quad \Rightarrow \quad q_2p = \frac{p^2}{2} \\
 q_2^2 &= (p + q_1)^2 = p^2 + q_1^2 + 2pq_1^2 \quad \Rightarrow \quad q_1p = -\frac{p^2}{2}
 \end{aligned} \tag{A.32}$$

Implementing these relations in the code can be realized with:

```
In[3]:= kinematics={q1.q1→m^2,q2.q2→m^2,q2.q1→m^2-p.p/2
                ,q_2.p→p.p/2,q1.p→-p.p/2};
```

With this setup, we can now start the computation of the nominators and denominators of Eqs. 3.3 and 3.29.

Photon Absorption from the Internal Scalar Line

The equation in question from Eq. 3.3 reads:

$$iM^\mu = q_H \cdot e \int_{\mathbb{R}^4} \frac{d^4k}{(2\pi)^4} \bar{u}(q_2) \frac{(c_s + c_p \gamma^5)(q_1 - \not{k} + m_F)(2k + p)(c_s^* - c_p^* \gamma^5)}{((q_1 - k)^2 - m_F^2 + i\varepsilon)((p + k)^2 - m_H^2 + i\varepsilon)(k^2 - m_H^2 + i\varepsilon)} u(q_1)$$

We start with the evaluation of the nominator. Here, we directly apply the substitution of $k \rightarrow k - yp + zq_1$. The function **FermionLineExpand** expands the products of Dirac matrices and automatically applies the Dirac equation and the Gordon identity.

```
In[4]:= Num1 = Simplify[FermionLineExpand[
    {u[q2,m], Cs 1+Cp γ5,
     γ.q1-γ.(k-yp+zq1)+ mF 1), 2(k-yp+zq1)_μ+p_μ,
     Conjugate[Cs] 1- Conjugate[Cp] γ5, u[q2,m]}
    /.p→q2-q1/.kinematics]]
```

As an output, we obtain a linear combination of all possible occurrences of Lorentz vectors. Since we are only interested in the extraction of the magnetic form factor that is proportional to $\sigma^{\mu\nu}p_\nu$. The relevant part from the output is:

```
Out[4]= iz(Cp(mF+m(-1+z))Conjugate[Cp] - Cs(m+mF-mz) Conjugate[Cs])
        {u[q2,m], σ_{μ,{-q1+q2}}, u[q1,m]}
```

Some rearranging allows us to obtain:

$$-iz(|Cp|^2 \underbrace{((1-z)m_\mu - m_F)}_{\zeta_-^\mu} + |Cs|^2 \underbrace{((1-z)m_\mu + m_F)}_{\zeta_+^\mu}) \sigma^{\mu\nu} p_\nu$$

where we can identify ζ_+^μ and ζ_-^μ as they were defined in Eq. 3.19. The denominator can be worked out as follows:

```
In[5]:= a=k.k-mH^2
        b=(p+k).(p+k)-mH^2
        c=(q1-k).(q1-k)-mF^2
        Den1=Simplify[Expand[x a+ y b+ c z+ iε/.x+y+z→1/./kin]]
```

```
Out[5]= iε - mH^2x - mH^2y + m^2z - mF^2z + (x+y+z)k.k + 2y k.p-2z k.q1 + yp.p
```

A Appendix

This results agrees exactly with the preliminary expression from Eq. 3.7. For the determination of Δ' (see calculation 3.10), we have:

$$\begin{aligned} \text{In}[6]:= & \text{Delta}=\text{Simplify}[\text{Expand}[\text{y}^2\text{p.p}-2\text{yz p.q1}+\text{z}^2\text{m}^2+ \text{mH}^2(1-\text{z})-\text{y p.p}-\text{z m}^2+\text{z mF}^2\sim 2 \\ & \text{/.kinematics/.x+y}\rightarrow 1-\text{z}]] \\ \text{Out}[6]= & -\text{mH}^2(-1+\text{z}) + (\text{mF}^2+\text{m}^2(-1+\text{z}))\text{z} + \text{y}(-1+\text{y}+\text{z})\text{p.p} \end{aligned}$$

which can be rearranged to

$$m_H^2(1-z) + (m_F^2 - m_\mu^2)z + m_\mu^2z - xyp^2$$

and confirms the result from Eq. 3.10.

Photon Absorption from the Internal Fermion Line

We can recall the invariant amplitude from Eq. 3.29

$$iM^\mu = -q_F e \int_{\mathbb{R}^4} \frac{d^4k}{(2\pi)^4} \bar{u}(q_2) \frac{(c_s + c_p \gamma^5)(\not{p} + \not{k} + m_F) \gamma^\mu (\not{k} + m_F)(c_s^* - c_p^* \gamma^5)}{((p+k)^2 - m_F^2 + i\varepsilon)((q_1 - k)^2 - m_H^2 + i\varepsilon)(k^2 - m_F^2 + i\varepsilon)}.$$

With the aforementioned substitution of $k^\mu \rightarrow k^\mu - yp^\mu + zq_1^\mu$, a simplification of the nominator can be obtained from:

$$\begin{aligned} \text{In}[7]:= & \text{Num2} = \text{Simplify}[\text{FermionLineExpand}[\\ & \langle \text{u}[q2,\text{m}], \text{Cs } 1+\text{Cp } \gamma 5, \\ & \gamma.\text{p}+\gamma.(k-y \text{ p}+z \text{ q1})+\text{mF } 1,\gamma_\mu,\gamma.(k-y \text{ p}+z \text{ q1})+\text{m}_F 1, \\ & \text{Conjugate}[\text{Cs}] 1- \text{Conjugate}[\text{Cp}] \gamma 5, \text{u}[q2,\text{m}] \rangle \end{aligned}$$

Extracting the relevant term results in:

$$\begin{aligned} \text{Out}[7]= & -i(-1+\text{z})(\text{Cp}(-\text{mF}+\text{m z})\text{Conjugate}[\text{Cp}]+\text{Cs}(\text{mF}+ \text{m z}) \text{Conjugate}[\text{Cs}]) \\ & \langle \text{u}[q2,\text{m}], \sigma_{\mu,\{-q1+q2\}}, \text{u}[q1,\text{m}] \rangle. \end{aligned}$$

These terms can be rearranged to:

$$i(1-z)(m_\mu z + m_F)|C_s|^2 + i(1-z)(m_\mu z - m_F)|C_p|^2 \quad (\text{A.33})$$

By taking a close look at the denominator by comparing Eqs. 3.29 and 3.3, we can see that we can swap $m_H \leftrightarrow m_F$ to obtain the result for the denominator in calculation. The required Δ_2 (index for the second scenario) is therefore given as:

$$\Delta_2 = -xyp^2 + m_\mu^2 z^2 + m_F^2(1-z) + (m_H^2 - m_\mu^2)z$$

We can now finalize the calculation in the same way as for the scalar interaction scenario, starting from Eq. 3.23, where the k integration is already carried out:

$$\begin{aligned} F_2^F(p^2) = & -\frac{q_H m_\mu^2}{8\pi^2} \int_0^1 dx dy dz \delta(x+y+z-1) \\ & \times \frac{(1-z)(|c_s|^2(z + \frac{m_F}{m_\mu}) + |c_p|^2(z - \frac{m_F}{m_\mu}))}{-xyp^2 + m_\mu^2 z^2 + m_F^2(1-z) + (m_H^2 - m_\mu^2)z}. \end{aligned}$$

From here we evaluate the integration over the Feynman parameters, apply the substitution $z' = 1 - z$ and set $p^2 \rightarrow 0$ following the same procedure as for the other topology to arrive at the expression:

$$F_2^F(0) = -\frac{q_F m_\mu^2}{8\pi^2} \int_0^1 dz' \frac{|c_s|^2(-z'^3 + z'^2 + \frac{m_F}{m_\mu} z'^2) + |c_p|^2(-z'^3 + z'^2 - \frac{m_F}{m_\mu} z'^2)}{m_\mu^2 z'^2 + m_H^2(1-z') + (m_F^2 - m_\mu^2)z'}$$

A Appendix

A.7 Explicit Calculation of the Mass Matrix

The masses of the individual particles can be obtained from the potential of Eq. A.35 by calculating the squared mass matrix given as:

$$M_{ij}^2 = \frac{\partial^2 V}{\partial \phi_i^\dagger \partial \phi_j} \quad (\text{A.34})$$

The potential is given as:

$$\begin{aligned} V = & m_{11}^2 H_1^\dagger H_1 + m_{22}^2 H_2^\dagger H_2 - \{m_{12}^2 (H_1^\dagger H_2 + H_2^\dagger H_1)\} \\ & + \frac{\lambda_1}{2} (H_1^\dagger H_1)^2 + \frac{\lambda_2}{2} (H_2^\dagger H_2)^2 + \lambda_3 (H_1^\dagger H_1)(H_2^\dagger H_2) \\ & + \lambda_4 (H_1^\dagger H_2)(H_2^\dagger H_1) + \frac{\lambda_5}{2} (H_1^\dagger H_2)^2 + \frac{\lambda_5^*}{2} (H_2^\dagger H_1)^2 \\ & + \lambda_6 (H_1^\dagger H_1)(H_1^\dagger H_2) + \lambda_6^* (H_2^\dagger H_1)(H_1^\dagger H_1) \\ & + \lambda_7 (H_2^\dagger H_2)(H_1^\dagger H_2) + \lambda_7^* (H_2^\dagger H_1)(H_2^\dagger H_2) \end{aligned} \quad (\text{A.35})$$

The eigenvalues of this matrix are then the masses of the the corresponding eigenstates. Hence we begin by utilizing the minimization conditions of the potential at which the doublet takes the VEV:

$$\left. \frac{\partial V}{\partial H_i} \right|_{\langle H_i \rangle = v_i} = 0 \quad (\text{A.36})$$

The explicit calculation yields for the first condition:

$$\begin{aligned} \frac{\partial V}{\partial H_1} = & M_{11}^2 H_1^\dagger + \dots + \frac{1}{2} \lambda_1 H_1^\dagger H_1^\dagger H_1 + \dots \stackrel{!}{=} 0 \\ \Rightarrow M_{11}^2 = & -\frac{\lambda_1}{2} v^2 \end{aligned} \quad (\text{A.37})$$

and for the second condition:

$$\begin{aligned} \frac{\partial V}{\partial H_2} = & \dots - M_{12}^2 H_1^\dagger + \dots + \lambda_6 H_1^\dagger H_1^\dagger H_1 \dots \stackrel{!}{=} 0 \\ \Rightarrow M_{11}^2 = & \frac{1}{2} \lambda_6 v^2 \end{aligned} \quad (\text{A.38})$$

All terms that remain proportional to H_2 or H_2^\dagger after the first derivative is taken are directly omitted as they equal zero because of the vanishing VEV of H_2 and H_2^\dagger . The minimization conditions can now be incorporated in A.35, from which the matrix elements are computed. The calculation is split up for the charged scalars and the neutral scalars. The matrix for the charged scalars has a 2x2 structure given as

$$M_{i,j}^2 = \frac{\partial^2 V}{\partial \phi_i \partial \phi_j} \quad \text{with} \quad \phi_i = G^+, H^+. \quad (\text{A.39})$$

Since Goldstone bosons get eaten up in the process of symmetry breaking, they do not acquire VEVs. For that reason, all matrix elements related to the Goldstone bosons become zero. The only non-vanishing matrix element will therefore be the M_{22}^2 element in the basis of $\{G^+, H^+\}$. Keeping in mind that all terms that remain proportional to H_2 and H_2^\dagger will vanish after taking the double derivative, we can only consider an effective potential V' for the purpose of this calculation.

$$\begin{aligned} V' = & M_{22}^2 (H_2^\dagger H_2) + \lambda_3 (H_1^\dagger H_1)(H_2^\dagger H_2) \\ = & M_{22}^2 (H^+ H^-) + \lambda_3 (H_1^\dagger H_1)(H^+ H^-) \end{aligned} \quad (\text{A.40})$$

Evaluating the derivative results in

$$M_{2,2}^2 = \frac{\partial^2 V}{\partial H^+ \partial H^-} = M_{22}^2 + \frac{\lambda_3}{2} v^2 \quad (\text{A.41})$$

A Appendix

turning the mass matrix in the basis $\{G^+, H^+\}$ into:

$$M^2 = \begin{pmatrix} 0 & 0 \\ 0 & M_{22}^2 + \frac{\lambda_3}{2}v^2 \end{pmatrix}. \quad (\text{A.42})$$

Since the matrix is already diagonalized, the condition for the mass of the charged scalar therefore reads

$$m_{H^+} = M_{22}^2 + \frac{\lambda_3}{2}v^2. \quad (\text{A.43})$$

We can now examine the mass matrix for the neutral scalars. Leaving out the cross terms, we can evaluate the upcoming dot products in the potential:

$$\begin{aligned} H_1^\dagger H_1 &= \frac{1}{2} (v^2 + H_1^0{}^2) \\ H_2^\dagger H_2 &= \frac{1}{2} ((H_2^0)^2 + (A^0)^2) \\ H_1^\dagger H_2 &= \frac{1}{2} (H_2^0(v + H_1^0) + iA^0(v + H_1^0)) \\ H_2^\dagger H_1 &= \frac{1}{2} (H_2^0(v + H_1^0) - iA^0(v + H_1^0)). \end{aligned} \quad (\text{A.44})$$

For the calculation of each matrix element, only the corresponding effective potential V' is considered. For M_{11}^2 we have:

$$\begin{aligned} V'_{11} &= M_{11}^2 (H_1^\dagger H_1) + \frac{1}{2} \lambda_1 (H_1^\dagger H_1)^2 \\ &\stackrel{\text{A.37, A.44}}{=} -\frac{1}{4} \lambda_1 v^2 (v^2 + (H_1^0)^2) + \frac{1}{8} \lambda_1 (v^4 + (H_1^0)^4). \end{aligned} \quad (\text{A.45})$$

Taking the derivative generates the following matrix entry:

$$\left. \frac{\partial^2 V'_{11}}{\partial H_1^0 \partial H_1^0} \right|_{\langle H_1^0 \rangle = v} = -\frac{1}{2} \lambda_1 v^2 + \frac{3}{2} \lambda_1 v^2 = \lambda_1 v^2. \quad (\text{A.46})$$

The same procedure is then applied for M_{22}^2 :

$$\begin{aligned} V'_{22} &= \frac{1}{2} M_{22}^2 ((H_2^0)^2 + (A^0)^2) + \frac{1}{2} \lambda_3 (H_1^\dagger H_1) ((H_2^0)^2 + (A^0)^2) \\ &\quad + \frac{1}{4} \lambda_4 ((H_2^0)^2 (v + H_1^0)^2 + (A^0)^2 (v + H_1^0)^2) \\ &\quad + \frac{1}{4} \lambda_5 ((H_2^0)^2 (v + H_1^0)^2 - (A^0)^2 (v + H_1^0)^2) \end{aligned} \quad (\text{A.47})$$

from which the matrix element can be calculated as:

$$\left. \frac{\partial^2 V'_{22}}{\partial H_2^0 \partial H_2^0} \right|_{\langle H_1^0 \rangle = 0} \stackrel{\text{4.3}}{=} M_{22}^2 + \frac{v^2}{2} (\lambda_3 + \lambda_4 + \lambda_5). \quad (\text{A.48})$$

The matrix element for M_{33}^2 can be calculated almost the same as for M_{22}^2 . The only difference is a minus sign in front of λ_5 which follows from taking the double derivative with respect to A^0 . All entries related to G^0 will vanish. In the basis of $\{H_1^0, H_2^0, A^0, G^0\}$ the squared mass matrix reads where the CP-conserving limit and the alignment limit have been utilized.

$$M^2 = \begin{pmatrix} \lambda_1 v^2 & 0 & 0 & 0 \\ 0 & M_{22}^2 + \frac{1}{2} v^2 (\lambda_3 + \lambda_4 + \lambda_5) & 0 & 0 \\ 0 & 0 & M_{22}^2 + \frac{1}{2} v^2 (\lambda_3 + \lambda_4 - \lambda_5) & 0 \\ 0 & 0 & 0 & 0 \end{pmatrix}. \quad (\text{A.49})$$

A Appendix

A.8 Left- and Right Handed Projection Operators

The idempotent left- and right handed operators are defined as [13]:

$$P_R = \frac{1}{2}(1 + \gamma^5) \quad \text{and} \quad P_L = \frac{1}{2}(1 - \gamma^5) \quad (\text{A.50})$$

with γ^5 given as:

$$\gamma^5 = \begin{pmatrix} -\mathbb{1} & 0 \\ 0 & \mathbb{1} \end{pmatrix}. \quad (\text{A.51})$$

They play an important role when it comes to the extraction of the left- or right-handed Weyl spinors (ψ_L or ψ_R) of a Dirac spinor ψ :

$$\psi = \begin{pmatrix} \psi_L \\ \psi_R \end{pmatrix}. \quad (\text{A.52})$$

Acting the projection operators on the Dirac spinor in the Weyl-basis obtains

$$P_L\psi = \psi_L \quad \text{and} \quad P_R\psi = \psi_R. \quad (\text{A.53})$$

References

- [1] S. Chatrchyan et al. “Observation of a new boson at a mass of 125 GeV with the CMS experiment at the LHC”. In: *Physics Letters B* 716.1 (Sept. 2012), pp. 30–61. ISSN: 0370-2693. DOI: 10.1016/j.physletb.2012.08.021. URL: <http://dx.doi.org/10.1016/j.physletb.2012.08.021>.
- [2] D.P. Aguillard et al. “Measurement of the Positive Muon Anomalous Magnetic Moment to 0.20ppm”. In: *Physical Review Letters* 131.16 (Oct. 2023). ISSN: 1079-7114. DOI: 10.1103/PhysRevLett.131.161802. URL: <http://dx.doi.org/10.1103/PhysRevLett.131.161802>.
- [3] T. Aoyama et al. “The anomalous magnetic moment of the muon in the Standard Model”. In: *Physics Reports* 887 (Dec. 2020), pp. 1–166. ISSN: 0370-1573. DOI: 10.1016/j.physrep.2020.07.006. URL: <http://dx.doi.org/10.1016/j.physrep.2020.07.006>.
- [4] M. Farhan, J. Julio, and J. S. Kosasih. “Explaining the muon $g - 2$ discrepancy by the two-Higgs-doublet model”. In: *J. Phys. Conf. Ser.* 2734.1 (2024), p. 012074. DOI: 10.1088/1742-6596/2734/1/012074.
- [5] G.C. Branco et al. “Theory and phenomenology of two-Higgs-doublet models”. In: *Physics Reports* 516.1–2 (July 2012), pp. 1–102. ISSN: 0370-1573. DOI: 10.1016/j.physrep.2012.02.002. URL: <http://dx.doi.org/10.1016/j.physrep.2012.02.002>.
- [6] Julian Schwinger. “On Quantum-Electrodynamics and the Magnetic Moment of the Electron”. In: *Phys. Rev.* 73 (4 Feb. 1948), pp. 416–417. DOI: 10.1103/PhysRev.73.416. URL: <https://link.aps.org/doi/10.1103/PhysRev.73.416>.
- [7] Hiren H. Patel. “Package-X: A Mathematica package for the analytic calculation of one-loop integrals”. In: *Computer Physics Communications* 197 (2015), pp. 276–290. ISSN: 0010-4655. DOI: <https://doi.org/10.1016/j.cpc.2015.08.017>. URL: <https://www.sciencedirect.com/science/article/pii/S0010465515003033>.
- [8] Friedrich Jegerlehner. *The Anomalous Magnetic Moment of the Muon, Second Edition*. ISBN: 978-3-319-63577-2. Springer International Publishing, 2017.
- [9] T. Albahri et al. “Measurement of the anomalous precession frequency of the muon in the Fermilab Muon $g - 2$ Experiment”. In: *Physical Review D* 103.7 (Apr. 2021). ISSN: 2470-0029. DOI: 10.1103/PhysRevD.103.072002. URL: <http://dx.doi.org/10.1103/PhysRevD.103.072002>.
- [10] Fred Jegerlehner and Andreas Nyffeler. “The muon $g2$ ”. In: *Physics Reports* 477.1–3 (June 2009), pp. 1–110. ISSN: 0370-1573. DOI: 10.1016/j.physrep.2009.04.003. URL: <http://dx.doi.org/10.1016/j.physrep.2009.04.003>.
- [11] Wolfgang Nolting. *Grundkurs Theoretische Physik 5/2*. e-ISBN: 978-3-642-24421-6. Springer International Publishing, 2017.
- [12] Francis Halzen and Alan D. Martin. *QUARKS AND LEPTONS: An Introductory Course in Modern Particle Physics*. e-ISBN: 978-3-642-24421-6. John Wiley Sons, Inc, 1984.
- [13] Matthew D. Schwartz. *Quantum Field Theory and the Standard Model, 1st ed.* ISBN: 978-1-107-03473-0. Cambridge University Press, 2014.
- [14] Jacques P. Leveille. “The Second Order Weak Correction to $(G-2)$ of the Muon in Arbitrary Gauge Models”. In: *Nucl. Phys. B* 137 (1978), pp. 63–76. DOI: 10.1016/0550-3213(78)90051-2.
- [15] Howard E. Haber and Gordon L. Kane. “The Search for Supersymmetry: Probing Physics Beyond the Standard Model”. In: *Phys. Rept.* 117 (1985), pp. 75–263. DOI: 10.1016/0370-1573(85)90051-1.
- [16] Ernest Ma. “Verifiable radiative seesaw mechanism of neutrino mass and dark matter”. In: *Phys. Rev. D* 73 (2006), p. 077301. DOI: 10.1103/PhysRevD.73.077301. arXiv: [hep-ph/0601225](https://arxiv.org/abs/hep-ph/0601225).
- [17] Lars Fromme, Stephan J. Huber, and Michael Seniuch. “Baryogenesis in the two-Higgs doublet model”. In: *JHEP* 11 (2006), p. 038. DOI: 10.1088/1126-6708/2006/11/038. arXiv: [hep-ph/0605242](https://arxiv.org/abs/hep-ph/0605242).

References

- [18] K. S. Babu and Sudip Jana. “Enhanced di-Higgs production in the two Higgs doublet model”. In: *Journal of High Energy Physics* 2019.2 (Feb. 2019). ISSN: 1029-8479. DOI: 10.1007/JHEP02(2019)193. URL: [http://dx.doi.org/10.1007/JHEP02\(2019\)193](http://dx.doi.org/10.1007/JHEP02(2019)193).
- [19] Sudip Jana, Vishnu P. K., and Shaikh Saad. “Resolving electron and muon $g - 2$ within the 2HDM”. In: *Phys. Rev. D* 101.11 (2020), p. 115037. DOI: 10.1103/PhysRevD.101.115037. arXiv: 2003.03386 [hep-ph].
- [20] The LEP Collaboration et al. *A Combination of Preliminary Electroweak Measurements and Constraints on the Standard Model*. 2004. arXiv: hep-ex/0312023 [hep-ex]. URL: <https://arxiv.org/abs/hep-ex/0312023>.
- [21] ATLAS Collaboration. *ATLAS searches for new particles in familiar decays*. <https://atlas.cern/Updates/Briefing/2HDM-Searches>. Retrieved, September 17, 2024. 2024.
- [22] Subhadip Bisal and Debottam Das. *Testing Z boson rare decays $Z \rightarrow H_1\gamma, A_1\gamma$ with $(g-2)_\mu$, M_W , and $BR(h_{\text{SM}} \rightarrow Z\gamma)$ in the NMSSM*. 2024. arXiv: 2308.06558 [hep-ph]. URL: <https://arxiv.org/abs/2308.06558>.
- [23] K. S. Babu, Sudip Jana, and Vishnu P. K. “Correlating W-Boson Mass Shift with Muon $g-2$ in the Two Higgs Doublet Model”. In: *Phys. Rev. Lett.* 129.12 (2022), p. 121803. DOI: 10.1103/PhysRevLett.129.121803. arXiv: 2204.05303 [hep-ph].
- [24] J. D. Bjorken et al. “Search for Neutral Metastable Penetrating Particles Produced in the SLAC Beam Dump”. In: *Phys. Rev. D* 38 (1988), p. 3375. DOI: 10.1103/PhysRevD.38.3375.
- [25] J. P. Lees et al. “Search for a muonic dark force at BaBar”. In: *Physical Review D* 94.1 (July 2016). ISSN: 2470-0029. DOI: 10.1103/physrevd.94.011102. URL: <http://dx.doi.org/10.1103/PhysRevD.94.011102>.
- [26] A.M. Sirunyan et al. “Search for an LL gauge boson using $Z \rightarrow 4\mu$ events in proton-proton collisions at $\sqrt{13\text{TeV}}$ ”. In: *Physics Letters B* 792 (May 2019), pp. 345–368. ISSN: 0370-2693. DOI: 10.1016/j.physletb.2019.01.072. URL: <http://dx.doi.org/10.1016/j.physletb.2019.01.072>.
- [27] T. Abe. *Belle II Technical Design Report*. 2010. arXiv: 1011.0352 [physics.ins-det]. URL: <https://arxiv.org/abs/1011.0352>.
- [28] Brian Batell et al. “Flavor-specific scalar mediators”. In: *Physical Review D* 98.5 (Sept. 2018). ISSN: 2470-0029. DOI: 10.1103/physrevd.98.055026. URL: <http://dx.doi.org/10.1103/PhysRevD.98.055026>.
- [29] H. Albrecht et al. “A search for the lepton-flavour violating decays $\tau \rightarrow e\alpha$, $\tau \rightarrow \mu\alpha$ ”. In: *Z. Phys. C - Particles and Fields* 68, 25–28 (1995). DOI: 10.1007/BF01579801.
- [30] Johannes Herms et al. “Minimal Realization of Light Thermal Dark Matter”. In: *Physical Review Letters* 129.9 (Aug. 2022). ISSN: 1079-7114. DOI: 10.1103/physrevlett.129.091803. URL: <http://dx.doi.org/10.1103/PhysRevLett.129.091803>.
- [31] Rahool Kumar Barman, Ritu Dcruz, and Anil Thapa. “Neutrino masses and magnetic moments of electron and muon in the Zee Model”. In: *Journal of High Energy Physics* 2022.3 (Mar. 2022). ISSN: 1029-8479. DOI: 10.1007/jhep03(2022)183. URL: [http://dx.doi.org/10.1007/JHEP03\(2022\)183](http://dx.doi.org/10.1007/JHEP03(2022)183).
- [32] S. Chatrchyan et al. “Observation of Z decays to four leptons with the CMS detector at the LHC”. In: *Journal of High Energy Physics* 2012.12 (Dec. 2012). ISSN: 1029-8479. DOI: 10.1007/jhep12(2012)034. URL: [http://dx.doi.org/10.1007/JHEP12\(2012\)034](http://dx.doi.org/10.1007/JHEP12(2012)034).
- [33] A. Hayrapetyan et al. “Search for the lepton-flavor violating decay of the Higgs boson and additional Higgs bosons in the $e\mu$ final state in proton-proton collisions at $\sqrt{S} = 13\text{TeV}$ ”. In: *Physical Review D* 108.7 (Oct. 2023). ISSN: 2470-0029. DOI: 10.1103/physrevd.108.072004. URL: <http://dx.doi.org/10.1103/PhysRevD.108.072004>.
- [34] Yoav Afik, P. S. Bhupal Dev, and Anil Thapa. “Hints of a new leptophilic Higgs sector?” In: *Physical Review D* 109.1 (Jan. 2024). ISSN: 2470-0029. DOI: 10.1103/physrevd.109.015003. URL: <http://dx.doi.org/10.1103/PhysRevD.109.015003>.

References

- [35] Steven Weinberg. *The Quantum Theory of Fields, Volume I*. Cambridge: Cambridge University Press, 2008, p. 497. ISBN: 978-0-521-67053-1.
- [36] Raimar Wulkenhaar. *Lecture Notes and Exercises on Integration Theory*. 2023.

Declaration of Academic Integrity

I hereby confirm that this thesis, entitled _____
_____ is solely my own work and
that I have used no sources or aids other than the ones stated. All passages in my thesis for
which other sources, including electronic media, have been used, be it direct quotes or content
references, have been acknowledged as such and the sources cited. I am aware that plagiarism
is considered an act of deception which can result in sanction in accordance with the
examination regulations.

(date, signature of student)

I consent to having my thesis cross-checked with other texts to identify possible similarities
and to having it stored in a database for this purpose.

I confirm that I have not submitted the following thesis in part or whole as an examination
paper before.

(date, signature of student)